



universität
wien

MASTERARBEIT

Titel der Masterarbeit

Latitudinal distribution and activity of prokaryotic
picoplankton populations in the North Atlantic Ocean

verfasst von

Franziska Maria Eibenberger, BSc

angestrebter akademischer Grad

Master of Science (MSc)

Wien, 2013

Studienkennzahl lt. Studienblatt: A 066 833

Studienrichtung lt. Studienblatt: Masterstudium Ökologie

Betreuer: Univ.-Prof. Dr. Gerhard Herndl

Einige Bücher darf man kosten,
andere muss man verschlingen,
und einige wenige kauen und verdauen.

Francis Bacon, 1597

I dedicate this thesis to all those,
who open this book and find, like me, what they have been searching for.

Franziska

Deutsche Zusammenfassung

Das prokaryotische Picoplankton beeinflusst maßgeblich die biogeochemischen Prozesse der Weltmeere, jedoch ist die Zusammensetzung dieser Lebensgemeinschaften sowie deren Verbreitung und Aktivitätsmuster weitestgehend unbekannt. Um einen besseren Einblick in die Diversität und Struktur des heterotrophen Picoplanktons zu bekommen, wurden im Rahmen dieser Arbeit die sechs abundantesten Bakterien- und Archaeen-Gruppen entlang eines Transekts über drei ozeanische Provinzen im Nordatlantik untersucht. Die gesamte Wassersäule bis in eine Tiefe von durchschnittlich 4000 m wurde beprobt und die relative Abundanz mittels Catalyzed Reporter Deposition Fluorescence in situ Hybridization (CARD-FISH) ermittelt, sowie die relative Aktivität mittels Mikroautoradiographie (Micro-CARD-FISH) erhoben. Generell dominierten Bakterien die Picoplanktongemeinschaft mit relativen Abundanzen zwischen 12-59%. Crenarchaeota waren zusammenfassend abundanter in der ozeanischen Provinz NADR (13-23%), im Gegensatz zu Euryarchaeota die einen Verbreitungsschwerpunkt in der ozeanischen Provinz NATR (15-31%) aufwiesen. Das Cluster SAR11 bildete die prozentuell häufigste bakterielle Gruppe mit relativen Abundanzen zwischen 11-31%, das bakterielle Cluster SAR202 stellte einen Anteil zwischen 5-23% und die Gruppe SAR324 stellte zwischen 2-15% der Picoplanktongemeinschaft dar. Die zellspezifische Aktivität von Bakterien und Crenarchaeota zeigte durchschnittlich die höchste relative Produktion in den Oberflächenschichten bei 100m (Bakterien $109 \text{ amol C cell}^{-1} \text{ d}^{-1}$, Crenarchaeota $48 \text{ amol C cell}^{-1} \text{ d}^{-1}$) und nahm gegen die Tiefe um bis zu drei Größenordnungen ab (Bakterien $12,1\text{-}0,1 \text{ amol C cell}^{-1} \text{ d}^{-1}$, Crenarchaeota $3,7\text{-}0,05 \text{ amol C cell}^{-1} \text{ d}^{-1}$).

Generell konnten keine eindeutigen Zonierungen nach Wassermassen beziehungsweise nach ozeanischen Provinzen für die relative Verbreitung der einzelnen Picoplanktongruppen oder für die Aktivitätsmuster von Bakterien und Crenarchaeota ermittelt werden.

Abstract

Prokaryotic picoplankton drive the main biogeochemical cycles in the ocean, but the specific distribution and activity of their members remain largely enigmatic. In order to determine the changes in picoplankton composition and activity from the base of the euphotic zone to the ocean's interior, we determined the distribution of major bacterial and archaeal groups along a transect across the North Atlantic spanning over three major oceanic provinces. Whole water column depth profiles were analyzed using catalyzed reporter deposition fluorescence in situ hybridization (CARD-FISH) to determine the abundance and CARD-FISH combined with microautoradiography (Micro-CARD-FISH) to determine the activity of individual prokaryotes. Generally, Bacteria dominated the picoplankton community and peaked in the center of the NASR in all water masses with relative abundances between 12-59%. The relative abundance of Crenarchaeota was higher in the NADR (2-27%) whereas in the NATR Euryarchaeota contributed between 15-31%. SAR11 was the most prominent bacterioplankton member with relative abundances of 11-31%, SAR202 ranged between 5-23% and SAR324 contributed only between 2-15%. On average, the cell-specific activity of Bacteria and Crenarchaeota was highest in the near surface layer (Bacteria $109 \text{ amol C cell}^{-1} \text{ d}^{-1}$, Crenarchaeota $48 \text{ amol C cell}^{-1} \text{ d}^{-1}$) decreasing by up to three orders of magnitude towards the ocean's interior (Bacteria $12.1\text{-}0.1 \text{ amol C cell}^{-1} \text{ d}^{-1}$, Crenarchaeota $3.7\text{-}0.05 \text{ amol C cell}^{-1} \text{ d}^{-1}$). Overall, our single cell data suggest that the abundance of the major prokaryotic groups and their cell-specific activity is similar among the individual deep-water masses and the oceanic provinces.

Table of Contents

1. Introduction	2
2. Material and Methods	6
3. Results	10
4. Discussion.....	14
5. Acknowledgements	19
6. Literature	20
7. Tables	24
9. Figures	27
10. Supplementary Information	34
10.1. Protocols	34
10.1.1. CARD-FISH.....	34
10.1.2. Micro-CARD-FISH.....	41
10.1.3. Microscopy and Evaluation.....	42
10.1.4. Chemicals and Preparations	43
10.2. Curriculum Vitae	53

1. Introduction

The Earth's most unique feature is its oceans that most decisively distinguish it from our neighboring planets. The oceans cover more than 72% of the Earth's surface and provide a vast environment thriving life. The oceans are a major driver of Earth's chemistry, climate and weather thereby providing cornerstones of the life-support on our planet (Field et al., 2002).

Prokaryotes (i.e., Bacteria and Archaea) are the main drivers of the biogeochemical cycles in the world's oceans (Azam et al., 1983; Karl, 2002) and form the basis of the food chain, being grazed upon by protists and lysed by viruses (Fenchel, 1986; Fuhrman, 1999). In contrast to the macroscopic organisms studied for centuries, the microscopic prokaryotes in the oceans received adequate attention only over the last forty years. Improvements in fluorescence microscopy and the introduction of DNA stains such as 4',6-diamidino-2-phenylindole (DAPI) in the 70s-80s made it possible to visualize the abundance of prokaryotes in seawater samples (Porter and Feig, 1980) and further developments, combining microautoradiography and fluorescence staining, facilitated unraveling the composition and activity of picoplankton communities in the sea (Teira et al., 2004).

The first deep-sea bacteria were isolated by ZoBell and colleagues in the 1930s and a relatively high abundance of prokaryotes in the oceans was assumed since the middle of the 20th century (ZoBell and Anderson, 1936). The first estimates of prokaryotic abundance in the oceans were underestimating its actual abundance by about three orders of magnitude. However, as these counts were derived from cultivation experiments of prokaryotes on agar plates and thus, did not represent the actual prokaryotic community, a phenomenon referred to as 'the great plate count anomaly' was reported (Jannasch and Jones, 1959). In fact, most of the oceanic microbes are not cultivable (Hugenholtz et al., 1998). Until the 1980s, prokaryotes were viewed as terminal decomposers with no or little contribution to biogeochemical cycling (Fenchel and Blackburn, 1979; Larsson and Hagström, 1979; Sorokin, 1981). Later, the introduction of the 'microbial loop hypothesis' highlighted the role of prokaryotes in the ocean's biogeochemical cycles emphasizing their importance as carbon link (or sink) in the oceanic food web (Azam et al., 1983). Microorganisms (e.g., Bacteria) convert dissolved organic carbon (DOC) released by the

phytoplankton into particulate organic carbon (POC), which, in turn, is grazed upon by protists. Thus, the microbial loop hypothesis suggests, that microorganisms channel energy and carbon effectively to the higher trophic levels (Fig. 1).

The phylogeny of marine prokaryotes is based on the 16S rRNA genes, pointing to a high diversity of marine Bacteria and Archaea (Giovannoni and Stingl, 2005). At the same time only a few phylogenetic groups are able to form large populations of >5% relative abundance because the members of the rare biosphere probably account for the majority of the microbial diversity (Sogin et al., 2006). Molecular tools in microbial oceanography substantially increased our knowledge on the community structure and function of marine picoplankton revealing that the vast majority of environmental microbes represent novel taxa that have yet to be cultivated (Handelsman, 2004).

Microbes are the most abundant group of organisms on our planet with an estimated cell abundance of $4\text{--}6 \times 10^{30}$ cells (Whitman et al., 1998). The oceanic water column alone hosts around 1×10^{29} cells and exhibiting high cell production rates amounting to 1.7×10^{30} cells yr^{-1} (Whitman et al., 1998). Microbes are abundant in all oceanic habitats, from the oceanic seafloor to the top millimeter of the ocean surface. Moreover, microbes thrive in environmental conditions where no other known organisms are present, from the cold brine channels of Arctic ice floes to hot waters of hydrothermal vents (Field et al., 2002). As a consequence of their diversity, marine microbes are involved in essentially all the geochemical reactions occurring in the oceans (Giovannoni and Stingl, 2005).

In the oceanic water column, microbial communities are vertically stratified (DeLong et al., 2006; Agogu   et al., 2011). Many of these microbial taxa are specialized to exploit vertical patterns in physical, chemical and biological parameters (Herndl et al., 2005; Teira et al., 2006; Schattnerhofer et al., 2009), which is in accordance with Baas Becking's theory of 'everything is everywhere but the environment selects' (Baas Becking, 1934). Recent studies using metagenomics provide new insight into the striking diversity and function of microorganisms in the environment (Morris et al., 2010; Agogu   et al., 2013; Allers et al., 2013). However, relatively few studies report on the activity and potential functional role of prokaryotes in the meso- and bathypelagic waters of the ocean.

The mesopelagic and bathypelagic realm of the ocean accounts for around 70% of the global oceans' volume (Field et al., 2002). The microbial biomass and activity decrease by one to two orders of magnitude from the euphotic layers to the bathypelagic realm and are extremely low in the dark ocean below 200 m depth (Patching and Eardly, 1997; Nagata et al., 2000; Hansell and Ducklow, 2003).

The oceans' epipelagic waters can be divided into several biogeographic provinces (Longhurst, 1998) with characteristic properties that might determine the dispersal and habitat of marine prokaryotes in the surface layers (Fig. 2). Individual prokaryotic species are not homogeneously distributed in the world's oceans because production and consumption of organic matter are dominated by local physical conditions, in turn, determining phytoplankton distribution and activity (Longhurst, 1998). Longhurst (1998) recognized four principal biomes present in the surface waters of the major oceans: the polar biome, the westerlies biome, the trade-wind biome and the coastal boundary-zone biome, which he divided further into several provinces. The oceanic provinces according to Longhurst (1998) demark areas with typical characteristics in turbulence, temperature, irradiance and nutrients and thus, form distinct pelagic surface water ecosystems. The boundaries of the individual provinces are not fixed in time and space but are dynamic systems that expand or retard due to seasonal and interannual changes in the abiotic and biotic parameters.

A meso- and bathypelagic classification into distinct provinces has not been investigated with scrutiny. Based on the distribution of pelagic metazoans, Brinton (1962) proposed a biogeographical classification into two mesopelagic provinces and one homogenous bathypelagic province (Fig. 3). Nevertheless, the dark ocean water mass circulation has not been taken into account in the scheme proposed by Brinton (1962). The pelagic ocean is not a homogenous water mass but consists of several water masses structured according to their density gradients (Fig. 4). The North Atlantic Deep Water (NADW), as a prominent example, is formed in the Greenland-Iceland-Norwegian Sea by sinking of highly saline and cold waters thereby transporting nutrients, oxygen and organic matter into the ocean's interior (Warren and Wunsch, 1981).

In this respect, the variability of picoplankton diversity across water masses and oceanic provinces has not been studied extensively. The general notion is, however, that non-sinking free-

living prokaryotes are trapped within distinct water masses, leading to a water mass-specific prokaryotic community composition and activity (Varela et al., 2008; Galand et al., 2010; De Corte et al., 2010). In the northern North Atlantic, bacterial assemblages from the subsurface, meso- and bathypelagic zones showed a clear clustering of microbial communities according to the water masses encountered (Agogue et al., 2011). Thus, the physical boundary conditions of deep-water masses might more restrict dispersal of free-living microbes than generally assumed.

The dark ocean microbial picoplankton depend on the rain of organic matter from the surface ocean suggesting that the distinct oceanic provinces and their specific variability in organic matter export are indicative for a distinct picoplankton community composition at depth. Despite reports indicating a relation of surface productivity and dark ocean prokaryotic biomass heterotrophic production exists in the Pacific (Nagata et al., 2000). It is currently unclear whether the Longhurst scheme (1998) of the surface ocean extends to the dark ocean.

In this study, we hypothesized that the prokaryotic community composition and its activity differ substantially between distinct water masses and according to oceanic provinces established by Longhurst (1998). To test this hypothesis, we followed a 3000-km-long transect from 48.75°N to 24.67°N occupying a total of 11 stations in three different oceanic provinces (Fig. 5). The focus of this study was to explore the distribution and activity of the major members of the heterotrophic prokaryotic community from the ocean's subsurface layer (> 100 m depth) to the ocean's interior using catalyzed reporter deposition fluorescence in situ hybridization (CARD-FISH) and CARD-FISH combined with microautoradiography (Micro-CARD-FISH). This allowed us to link the distribution and activity patterns with physico-chemical parameters.

Our analysis suggests that the distribution of the major prokaryotic groups is similar in all major water masses of the southern North Atlantic. Additionally, the relative abundance and activity of the major prokaryotic groups of the dark North Atlantic does not seem to cluster according to the oceanic provinces introduced by Longhurst (1998).

2. Material and Methods

Study sites and sampling

During the MEDEA 1 cruise in October-November 2011 the eastern branch of the North Atlantic Deep Water was followed over a 3000-km-long transect on board of the Dutch R/V *Pelagia*. The cruise followed a transect from 48.75°N, 22.51°W to 24.67°N, 34.94°W with a total of 11 stations occupied (Fig. 5). Water samples were collected with a conductivity-temperature-depth (CTD) rosette sampler holding 19 Niskin bottles of 25 L each. At each station, six different water layers were sampled including the lower end of the euphotic layer (100 m) at around 100 m depth, the oxygen minimum layer (O₂-min) at around 250 m depth, the Mediterranean Sea Outflow Water (MSOW) at 1000 m depth, the Antarctic Intermediate Water (AAIW) at 1800 m depth, the North East Atlantic Deep Water (NADW) at 2750 m depth and the Lower Deep Water (LDW) at 4000 m depth. The water masses were identified based on their salinity-temperature characteristics (van Aken 2000).

The oxygen concentrations were measured using a Seabird SBE43 oxygen sensor mounted on the frame of the CTD. At each depth, samples were taken to determine the concentrations of the inorganic nutrients, the prokaryotic abundance (PA), the prokaryotic heterotrophic production and the relative abundance and activity of heterotrophic prokaryotes using catalyzed reporter deposition fluorescence in situ hybridization (CARD-FISH) and CARD-FISH combined with microautoradiography (Micro-CARD-FISH).

Biogeographical provinces

According to the latitudinal position of the thermohaline properties and in agreement with the classification proposed by Longhurst (1998) four major oceanic provinces could be distinguished and were further defined for this study according to the net primary production rate (NPP) at the particular sites. The NPP was determined via satellite images taken during the cruise and was calculated according to the vertically generalized production model (VGPM) established by Behrenfeld and Falkowski (1997). The North Atlantic drift region (NADR) was defined with a NPP of 500-1000 mg C m⁻² d⁻¹, the Northeast Atlantic subtropical region (NASE) and the

Northwest Atlantic subtropical region (NASW) with an NPP between 200-300 mg C m⁻² d⁻¹ and the North Atlantic tropical gyre region (NATR) with an NPP lower than 200 mg C m⁻² d⁻¹. The Northeast Atlantic subtropical region (NASE) and the Northwest Atlantic subtropical region (NASW) are referred to as the North Atlantic subtropical region (NASR) in this study. The stations sampled in these oceanic provinces are shown in Fig. 5.

Inorganic nutrients

The concentrations of inorganic nutrients (NH₄⁺, NO₃⁻, NO₂⁻, PO₄³⁻, SiO₄⁻) were determined immediately after collecting the samples via gentle filtration through 0.2-mm filters (Acrodisc, Gelman Science) in a TRAACS autoanalyzer system. Ammonium [NH₄⁺] was detected with the indophenol blue method (pH 10.5) at 630 nm (Helder and Vries, 1979). Nitrate [NO₃⁻] was reduced in a copper cadmium coil to nitrite (with imidazole as a buffer) and then measured as nitrite. Nitrite [NO₂⁻] was determined after diazotation with sulfanilamide and N-(1-naphtyl)-ethylene diammonium-dichloride as the reddish-purple dye complex at 540 nm (Parsons et al., 1984). Phosphate [PO₄³⁻] was determined via the molybdenum blue complex at 880 nm according to Murphy and Riley (1962).

Prokaryotic abundance

One mL seawater samples were fixed with 37% formaldehyde (2% final conc.), stained with 0.5 mL of SYBRGreen I (Molecular Probes) at room temperature in the dark for 15 min, and subsequently analyzed on a FACSCalibur flow cytometer (BD Biosciences) (Lebaron et al., 1998). Counts were performed with the argon laser at 488 nm wavelength set at an energy output of 15 mW. The prokaryotic cells were enumerated according to their right-angle light scatter and the green fluorescence was measured at 530 nm. High nucleic acid (HNA) prokaryotes were distinguished from low nucleic acid cells in the side scatter *versus* green fluorescence plot where HNA populations show higher fluorescence compared to low nucleic acid (LNA) cells.

Leucine incorporation as a proxy of heterotrophic prokaryotic production

Bulk prokaryotic activity was measured by incubating 10-80 mL of water in duplicate and one formaldehyde-killed blank with 10 nmol L⁻¹ [³H]-leucine (Specific activity 120 Ci mmol⁻¹) in the

dark at in situ ($\pm 1^{\circ}\text{C}$) temperature for 4–7 h, depending on the expected activity. Thereafter, the incubation was terminated by adding 37% formaldehyde (2% final conc.) to the samples. After 10 min, the samples were filtered through 0.2- μm polycarbonate filters supported by cellulose nitrate filters (Millipore, 25-mm filter diameter). Subsequently, the filters were rinsed three times with 5% ice-cold trichloroacetic acid, placed in scintillation vials, and stored at -20°C until counting in a liquid scintillation counter. The disintegrations per minute (DPM) of the formaldehyde-fixed blank were subtracted from the mean DPM of the duplicate sample, and the resulting DPM were converted into leucine incorporation rates. The leucine incorporation was converted into prokaryotic carbon biomass production using the theoretical conversion factor and assuming a 2-fold isotope dilution. Hence a conversion factor of $3.1 \text{ kg C mol}^{-1}$ leucine was applied (Simon and Azam, 1989).

Catalyzed fluorescence in situ hybridization and microautoradiography

Depending on the sampling depth, water samples of 20–80 mL were fixed by adding 0.2- μm filtered paraformaldehyde (2% final conc.), and, subsequently, the samples were stored at 4°C in the dark for 12–18 h. Thereafter, the samples were filtered through a 0.2- μm polycarbonate filter (Millipore, GTTP, 25-mm filter diameter) supported by a cellulose nitrate filter (Millipore, HAWP, 0.45 μm), washed twice with fresh Milli-Q water, and dried and stored at -80°C in a microfuge tube until further processing in the home laboratory.

Filters for CARD-FISH and Micro-CARD-FISH were embedded in low melting point agarose and incubated either with lysozyme (50000 U mg^{-1} , Sigma-Aldrich), for the bacterial probes and for the negative control probe Non338, or were incubated with proteinase-K ($>800 \text{ U mL}^{-1}$, Sigma-Aldrich), for the archaeal probes. Different horseradish peroxidase (HRP) oligonucleotide probes were used to target either the Bacteria (EUB338 I, EUB338 II, EUB338 III) the bacterial cluster SAR11 (SAR11-152R, SAR11-441R, SAR11-542R, SAR11-732R), the bacterial clade SAR406 (SAR406-97), the bacterial clade SAR324 (SAR324-625, helper), the bacterial cluster SAR202 (SAR202-104R, SAR202-312R), or the archaeal divisions Crenarchaeota (CREN537, CREN554) and Euryarchaeota (EURY806). Hybridization and tyramide amplification was done following the protocol described in Teira et al. (2004). After the hybridization the Micro-

CARD-FISH filters were exposed to photographic emulsion (Type NTB-2, KODAK) in the dark for 7 days and then developed (Dektol developer, KODAK) and fixed (fixer, KODAK). On the CARD-FISH filters, cells were counterstained with a 4',6-diamidino-2-phenylindole and afterwards mounted in a Citifluor-Vectashield-mix onto slides. The Micro-CARD-FISH filters were directly counterstained and mounted in a DAPI-mix onto slides.

The slides were examined under a Zeiss Axiovision microscope equipped with a 120 W metal halid lamp (HXP 120C) and appropriate filter sets for DAPI, Alexa488 and transmission light. In 10 or more regions of interest (ROI) more than 400 DAPI-stained cells were counted via a digital image analysis and counting system (Frank et al., in prep). In each ROI up to four different categories were enumerated: (1) total DAPI-stained cells, (2) DAPI-cells additionally stained with the specific probe, and additionally for Micro-CARD-FISH (3) DAPI-cells and DAPI-probe-cells with silver grain halo around the cell and (4) the area of the halo area. Negative control counts (hybridization with Non338) were always below 1% of DAPI-stained cells. The counting error, expressed as the percentage of standard error between replicates, was 25% for DAPI counts and, 7% for FISH counts. A more detailed protocol on the CARD-FISH and Micro-CARD-FISH method is given in the Supplementary Information.

Statistical analysis

ANOVA was used for the mean comparison of the distribution according to water mass or oceanic province. For correlation analysis, the Spearman coefficient was used. The non-parametric Mann-Whitney-U-test was used for mean comparison of two independent samples, if normality was not attained.

3. Results

Water mass characteristics

The physical and chemical characteristics of the main water masses encountered along the transect, averaged within each of the three oceanic provinces, are summarized in Table 1. At around 4000 m depth, the LDW was characterized by the low temperatures between 2.91-3.15°C and high nitrate concentration of $\sim 19.5 \mu\text{mol L}^{-1}$. The core of the NADW was found at around 2750 m depth. The NADW was characterized by a salinity of ~ 34.9 and a temperature of $\sim 3^\circ\text{C}$. The AAIW was found at ~ 1800 m depth and the MSOW was sampled at ~ 1000 m depth. The MSOW is characterized by relatively high salinity of 35.3 and relatively high temperature of $\sim 7^\circ\text{C}$. The O_2 -min at ~ 250 m depth was characterized by apparent oxygen utilization (AOU) concentrations ranging between 72.9-115.5 $\mu\text{mol L}^{-1}$.

Nitrate decreased two orders of magnitude within the 100 m depth horizon towards the south with the lowest concentration measured ($0.01 \mu\text{mol L}^{-1}$) in the NATR, whereas in the water layers below 1000 m the nitrate concentrations increased towards the NATR ranging between 17.8-22.8 $\mu\text{mol L}^{-1}$. Silicate and AOU showed similar patterns as nitrate with decreasing concentrations in the 100 m depth horizon towards the south and increasing concentrations in the meso- and bathypelagic layers towards the NATR (Table 1).

Prokaryotic abundance and heterotrophic activity

PA, HNA, total leucine incorporation and the cell-specific production rate are shown in Table 2. Prokaryotic abundance decreased exponentially with depth from 100 m to 4000 m. PA and HNA cells were significantly different between the surface waters and the deep-water layers (ANOVA, $n = 18$, $p < 0.01$). The relative abundance of HNA cells was higher in the mesopelagic layers of the NADR and NATR as compared to that in the NASR. Leucine incorporation decreased with depth by one order of magnitude in the NADR and three orders of magnitude in the NATR and overall ranged from $0.2 \text{ pmol Leu L}^{-1} \text{ d}^{-1}$ to $82.1 \text{ pmol Leu L}^{-1} \text{ d}^{-1}$ (Fig. 6a). Leucine incorporation was lowest in the waters below 1000 m of the NATR ($0.04 \text{ pmol Leu L}^{-1} \text{ d}^{-1}$), whereas the highest leucine incorporation was measured in the

100 m layer of the NATR with $168.7 \text{ pmol Leu L}^{-1} \text{ d}^{-1}$. The cell-specific production ranged from $53.3 \text{ amol C cell}^{-1} \text{ d}^{-1}$ in the 100 m layer to $\sim 2.1 \text{ amol C cell}^{-1} \text{ h}^{-1}$ in the deep waters (Fig. 6b). In the 100 m layer, the cell-specific production increased by one order of magnitude towards the NATR ($100.6 \text{ amol C cell}^{-1} \text{ d}^{-1}$) and was lowest in the LDW of the NATR province ($0.9 \text{ amol C cell}^{-1} \text{ d}^{-1}$).

Prokaryotic community composition

The mean contribution of Bacteria, Crenarchaeota and Euryarchaeota to the total prokaryotic abundance of the different water layers and water masses as well as for the oceanic provinces along the transect are given in Fig. 7. The sum of the CARD-FISH positive Bacteria, Crenarchaeota and Euryarchaeota averaged $61 \pm 12\%$ ($n = 54$) of the DAPI-stained cells (Fig. 7). Overall, the bacterial fraction of the DAPI-stained cells varied between 12-59%, the contribution of Crenarchaeota varied between 2-27%, while Euryarchaeota contributed between 1-31% to the total abundance of DAPI-stained cells. The relative bacterial abundance was highest throughout the water column at the central station of the NASR (Fig. 7). Bacteria contributed significantly less to the prokaryotic abundance in the water column of the NATR (ANOVA, $n = 6$, $p < 0.01$). Crenarchaeota significantly decreased in relative abundance from the NADR towards the NATR throughout the water column (ANOVA, $n = 6$, $p < 0.01$). Generally, Crenarchaeota exhibited the highest relative abundance in all three provinces in the LDW contributing $\sim 16\%$ to the total prokaryotic abundance. The percentage of Euryarchaeota increased significantly in the NATR compared to the other provinces (ANOVA, $n = 6$, $p < 0.01$) and averaged $\sim 12\%$ in the LDW. Overall, a general trend in the relative abundances of Bacteria, Crenarchaeota and Euryarchaeota for the different water masses or oceanic provinces was not apparent along the transect (Fig. 7).

The sum of the relative abundances of SAR11, SAR324, SAR202, Crenarchaeota and Euryarchaeota averaged $54 \pm 7\%$ ($n = 90$) of the total DAPI-stainable cells (Fig. 8). SAR11 contributed between 11-31% to the total prokaryotic abundance, SAR324 contributed between 1-15%, and SAR202 contributed between 5-23%. The relative abundance of SAR11 and SAR324 was highest in the NADW (SAR11 $\sim 24\%$ and SAR324 $\sim 8\%$), whereas SAR202 and Euryarchaeota reached the highest relative abundances in the LDW (SAR202 $\sim 13\%$ and Euryarchaeota $\sim 14\%$). SAR324 and Euryarchaeota contributed significantly more to the total prokaryotic abundance in

the NATR (ANOVA, $n = 6$, $p < 0.01$) than in the NADR, particularly in the deeper water column (AAIW to LDW). Crenarchaeota exhibited the highest relative abundance in the O₂-min and the LDW with ~13% in both water masses. The relative abundance of Crenarchaeota was significantly lower in the water column of the NATR (ANOVA, $n = 6$, $p < 0.01$). The percentage of SAR202 and SAR11 did not show any significant trends over the oceanic provinces.

Group specific single-cell activity based on Micro-CARD-FISH analysis

The cell-specific production of Bacteria and Crenarchaeota was calculated via the relative leucine incorporation of the probe-positive cells and converted into specific production using the theoretical conversion factor by Simon and Azam (1989). Generally the cell-specific production of Bacteria and Crenarchaeota was highest in the 100 m layer and decreased by two orders of magnitude towards the ocean's interior (Fig. 9). The cell-specific production of Bacteria ranged between 1.1-127.6 amol C cell⁻¹ d⁻¹, with a maximum in the 100 m layer of ~109 amol C cell⁻¹ d⁻¹ on average. In the 100 m layer, the cell-specific production of Bacteria increased along the transect from the NADR towards the NATR by 38 amol C cell⁻¹ d⁻¹ (Fig. 9). In the ocean's interior, however, the cell-specific bacterial production decreased along the transect towards the NATR by one to two orders of magnitude (12.1-0.1 amol C cell⁻¹ d⁻¹). The cell-specific production based on the relative abundance of Crenarchaeota ranged between 0.05-85.6 amol C cell⁻¹ d⁻¹ with a maximum in the 100 m layer of 48.3 amol C cell⁻¹ d⁻¹ on average. Towards the NATR, the cell-specific production of Crenarchaea decreased by up to three orders of magnitude averaging 0.8 amol C cell⁻¹ d⁻¹ (Fig. 9). Crenarchaeal cell-specific production below 250 m depth peaked in the oxygen minimum layer and the LDW. In general, the bacterial and crenarchaeal single cell production were higher in the surface waters compared with to the water layers below 250 m depth, and additionally were higher in the NADR than in the other two oceanic provinces, but, however, no significant trend could be observed.

Environmental factors and prokaryotic community structure and function

The relationship between the contribution of the major prokaryotic groups and the main environmental variables was analyzed (Table 3). Overall, the relative abundance of Bacteria and

SAR202 was correlated with each of the tested parameters. The relative abundance of Bacteria was generally positively correlated with the environmental and microbial parameters, only with nitrate and AOU bacterial abundance was negatively related. The relative abundance of SAR202 was negatively correlated with the environmental parameters, except for nitrate and AOU (Table 3). The relative abundance of SAR11 showed a single negative correlation with AOU. The relative abundance of SAR324 was positively correlated with nitrate and negatively with PA, HNA, leucine incorporation and cell-specific production. The relative abundance of Euryarchaeota was positively correlated with nitrate and negatively with the cell-specific production. Both bacterial and crenarchaeal cell-specific production were positively correlated with the general cell-specific production and additionally, the crenarchaeal cell-specific production was positively correlated with the percentage of HNA cells.

4. Discussion

Data quality

The overall coverage of the prokaryotic community, given as the sum of the relative abundance of Bacteria, Crenarchaea and Euryarchaea averaged $60 \pm 13\%$ and was well within the total recovery efficiency documented previously (Teira et al., 2006; Schattenhofer et al., 2009). The enumeration via our digital image analysis and counting system ensured objective and consistent data analysis with higher sensitivity than compared to conventional counting (Frank et al., in prep). However, the variable recovery efficiency of the probes targeting bacterial and archaeal groups suggests dormant or dead cells with an extremely low rRNA content, impermeable cells or cells with mutations at the probe target site (Schattenhofer et al., 2009).

We additionally hybridized filter section with the HRP probe SAR406-97 (Fuchs et al., 1997) targeting the Marine Group A (MGA) bacteria. The relative abundance of the MGA bacteria outnumbered the recently documented contributions of 1-9% and was in our study 6-45% (Schattenhofer et al., 2009; Allers et al., 2013). For CARD-FISH, we hybridized with a hybridization buffer containing 65% formamide at a hybridization temperature of 35°C in contrast to other studies where MGA bacteria were hybridized in a buffer with 40% formamide at 46°C (Schattenhofer et al., 2009; Allers et al., 2013). Thus, despite similar hybridization conditions our higher formamide concentration should compensate the higher temperature used in the above-mentioned studies, unspecific binding of the probe might have resulted in a higher abundance of MGA bacteria in our study. Consequently, the data of the MGA bacteria were not analyzed due to the questionable data quality.

Distribution of Bacteria

The relative abundance of Bacteria enumerated by the probe mix EUBI-III ranged between 15-59% with the lowest relative abundance in the 100 m depth layer (Fig. 7). The low relative abundance of EUB-positive cells does not appear to result from poor cell lysis, as a lysis comparison performed by Pernthaler and colleagues (2004) using lysozyme and achromopeptidase revealed no significant

differences. Moreover, Teira and colleagues (2004) showed with a comparison of the recovery of DAPI-stained cells before and after the CARD-FISH procedure insignificant differences in cell abundances indicating negligible cell losses from the filter sections during sample treatment. Overall, however, the yield of EUB-positive cells was in the range of other reports from different oceanic regions (Allers et al., 2013). The relative contribution of Bacteria to the total prokaryotic abundance lacked significant depth related trends (Fig. 7). The contribution of Bacteria to the total prokaryotic abundance has been shown to decrease towards the interior of the ocean by one order of magnitude, with higher abundances in the surface layers of the temperate, polar regions and upwelling regions of the open ocean than in tropical regions (Schattenhofer et al., 2009; Teira et al., 2006).

Distribution of the SAR clusters

The SAR11 cluster dominated the bacterial community throughout the water column and showed a maximum in the NADW of the NADR (Fig. 8). This deep maximum of the SAR11 may suggest transport of these cells from the formation region of the NADW into the deep North Atlantic basin. Furthermore, the negative correlation of SAR11 with AOU supports the hypothesis that SAR11 in deep waters is linked to generally young deep waters (Table 3). In a similar transect, the SAR11 cluster was found to dominate the ocean surface layers (Schattenhofer et al., 2009) and may also account for the majority of the mesopelagic picoplankton (Morris et al. 2002). Other reports show a strong relation of SAR11 to reduced sulfur compounds like Dimethylsulfoniopropionate (DMSP) from phytoplankton (Stefels et al., 2000). Thus, a positive relationship of SAR11 with the primary production rate might exist with higher relative abundances in regions of higher primary production rates. However, the relative abundances of the SAR11 in the surface waters of the productive NATR and oligotrophic NADR were similar, indicating that other mechanisms of dispersal might also play a role (Fig. 8). SAR11 is known to be highly competitive for limiting substrates compensating the limited availability of certain nutrients with enhanced uptake efficiency resulting in a rather homogeneous dispersal over oligotrophic and eutrophic oceanic regions (Mary et al., 2006).

The SAR324 cluster increased in relative abundance towards the deeper layers of the water column and towards the south (Fig. 8) which is in line with previous studies (Gordon and Giovannoni, 1996). Moreover, the relative abundance of SAR324 was positively correlated with nitrate (Table 3). Recent studies identified that the SAR324 cluster might be preferentially attaching to particles with the potential to fix inorganic carbon and use sulfur- and methane as an energy source (Swan et al., 2011).

The Chloroflexi-like SAR202 cluster lacked a significant trend related to the different water layers and oceanic provinces but the depth related correlation with the main environmental parameters (Table 3) indicating that members of the SAR202 cluster are not ubiquitously distributed in the water column (Fig. 8). Varela et al. (2008) documented an increasing abundance of the Chloroflexi-type SAR202 cells in the (sub)tropical Atlantic from the surface layers (1%) towards the mesopelagic zone with constant relative abundances down to 4000 m depth (10-20%). This suggests that these Bacteria are well adapted to exploit the bathypelagic realm. Further, the SAR202 abundance was reported to correlate with oxygen (Giovannoni et al., 1996). The Chloroflexi-like SAR202 cluster, being particularly abundant in the deep waters of the Atlantic has been shown to take up only L-amino acids which is rather surprising since generally deep-water prokaryotes are efficient in taking up D-amino acids (Varela et al, 2008).

Distribution of Cren- and Euryarchaeota

Towards the deeper water layers Crenarchaea generally increase in relative abundance indicating their potentially important role in the meso- and bathypelagic waters (Karner et al., 2001). Knowledge on the ubiquitous distribution of Archaea in the marine pelagic realms is relatively recent and the factors controlling the dispersal of the major archaeal groups in the oxygenated water column of the ocean remain largely unknown (DeLong et al., 1994; Teira et al., 2006). Recent studies reported a sharp increase of crenarchaeal abundance in the oxygen minimum layer and documented the involvement of, at least, some members of the Crenarchaeota in nitrogen cycling, particularly in the oxidation of ammonia (Wuchter et al., 2006; Treusch et al., 2006). As all known ammonia-oxidizing prokaryotes are fixing inorganic carbon as a carbon source, this

metabolic feature has been used to assess their biomass production (Herndl et al. 2005; Varela et al., 2011). In general, our results confirm the previously documented distribution patterns of Crenarchaeota and Euryarchaeota with depth (Fig. 7, Fig. 8), albeit, along our transect we could not find a significant difference between distinct water masses or oceanic provinces.

Distribution according to the oceanic provinces (Longhurst, 1998)

The relative abundance of Bacteria in the NASR and NADR was similar while it was significantly lower in the NATR (Fig. 7). Similarly to the bacterial abundance scheme, the relative abundance of the SAR324 cluster and Euryarchaeota was significantly different between the NADR/NASR and the NATR. The NASR and the NATR both belong to the North Atlantic Gyral Province and are separated from the NADR by the northeasterly flow of the North Atlantic Current (Longhurst, 1998). Consequently, one would expect that the bacterial community of the NASR and NATR province should be more similar and both of them more different from the bacterial community of the NADR province. However, there is a trophic gradient from N-S which might have caused these changes in the relative abundance of the SAR324 cluster and the Euryarchaea from NADR /NASR to NATR.

Cell-specific activity

The cell-specific production patterns of Bacteria and Crenarchaeota, estimated via the relative leucine uptake and converted to carbon units, was generally highest in the surface waters with a peak in the NADR and decreasing towards the ocean's interior with the lowest cell-specific production measured in the NATR (Fig. 9). The decreasing cell-specific activity from the northern to the southern province reflects the decreasing surface water productivity. The cell-specific bacterial production (calculated via the relative leucine incorporation of the EUB positive cells) remained rather stable in the 100 m depth horizon, whereas the cell-specific crenarchaeal production was lowest in the surface waters of the NATR (Fig. 9). In the deep waters, Crenarchaea exhibited the lowest cell-specific production in the AAIW at all three provinces and higher cell-specific production again towards the shallower waters up to 250 m as well as towards the

bathypelagic water masses (Fig. 9). This cell-specific leucine incorporation pattern indicates enhanced crenarchaeal activity in the oxygen minimum zones and the bathypelagic waters.

The activity measurements were made under surface-pressure conditions, however, decompression of the sample water collected from 4000 m depth prior to the incubation might alter the prokaryotic activity (Herndl et al., 2005). It remains to be shown how changing hydrostatic pressure affects the activity of individual prokaryotic groups when measurements are done at surface pressure conditions as performed in this study.

Summary and conclusions

While changes in the heterotrophic prokaryotic community composition between different stations and depth were detectable, no distinct trends were observable. This is surprising since next generation sequencing and fingerprinting techniques do reveal water mass-specificity of the bacterial community as well as depth stratification. It might be that the probes we were using were too coarse to identify changes in the community compositions. Future studies using FISH probes targeting more specific prokaryotic groups, in combination with next generation sequencing techniques will provide deeper insights into the prokaryotic community composition of the North Atlantic.

5. Acknowledgements

I thank my supervisor Prof. G. J. Herndl and my co-supervisor T. Reinthaler for making this Master Thesis possible and for their help during the design and in the writing phase of the thesis. I especially thank my hands-on supervisor A. Frank for his patient assistance in the lab explaining all the methods and his valuable feedback in the data analyses. Further, I thank C. Baranyi for his support in the lab and all the members of the oceanography section of the Dept. of Limnology and Oceanography for their feedbacks and for making the lunch breaks so enjoyable. Last but not least, I greatly thank my grand family, my lovely friends and my brilliant fellow students for their patient support and constructive help during the time of my master thesis. This work was supported by the FWF grant PADOM (P23221-B11) to T. Reinthaler and by FWF projects I486-B09 and P23234-B11 and the ERC advanced Grant MEDEA to G. J. Herndl.

6. Literature

- Agogu , H., Lamy, D., Neal, P.R., Sogin, M.L., Herndl, G.J., 2011. Water mass- specificity of bacterial communities in the North Atlantic revealed by mas- sively parallel sequencing. *Mol. Ecol.* 20, 258–274
- Allers, E., Wright, J.J, Konwar, K.M., Howes, C.G, Beneze, E. Hallam, S.J., and Sullivan, M.B. (2013) Diversity and population structure of Marine Group A bacteria in the Northeast subarctic Pacific Ocean. *ISME J.*, 7(2), pp.256–68.
- Amann, R.I., Binder, B.J., Olson, R.J., Chisholm, S.W., Devereux, R., and Stahl, D.A. (1990) Combination of 16S ribosomal-RNA-targeted oligonucleotide probes with flowcytometry for analyzing mixed microbial populations. *Appl. Environ. Microbiol.* 56: 1919–1925
- Azam, F., Fenchel, T., and Field, J.G. (1983) The Ecological Role of Water-Column Microbes in the Sea. *Mar. Ecol. Prog. Ser.* 10:257–263.
- Baas Becking, L.G.M. (1934) *Geobiologie of Inleiding tot de Milieukunde*. The Hague, the Netherlands.
- Behrenfeld, M.J., and Falkowski, P.G. (1997) Photosynthetic rates derived from satellite-based chlorophyll concentration. *Limnol. Oceanog.* 42:1-20.
- Daims, H., Br hl, A., Amann, R., Schleifer, K.H., and Wagner, M. (1999) The domain-specific probe EUB338 is in- sufficient for the detection of all bacteria: Development and evaluation of a more comprehensive probe set. *System. Appl. Microbiol.* 22: 434–444.
- De Corte, D., Sintes, E., Winter, C., Yokokawa, T., Reinthaler, T., and Herndl, G.J. (2010) Links between viral and prokaryotic communities throughout the water column in the (sub)tropical Atlantic Ocean. *ISME J.* 4(11), pp.1431–42.
- DeLong, E.F., Wu, K.Y., Prezelin, B.B., and Jovine, R.V.M. (1994) High abundance of Archaea in Antarctic marine picoplankton. *Nature* 371:695–697.
- DeLong, E.F., Preston, C.M., Mincer, T., Rich, V., Hallam, S.J., Frigaard, N.U., et al. (2006) Community genomics among stratified microbial assemblages in the ocean's interior. *Science* 311: 496–503.
- Fenchel, T., and Blackburn, T.H. (1979) *Bacteria and mineral cycling*. Academic Press. London.
- Fenchel, T. (1986) The ecology of heterotrophic microflagellates. *Adv. Mic. Ec.* 9:57–97.
- Field, J.G, Hempel, G., and Summerhayes, C.P. (2002) *Oceans 2020: Science, Trends, and the Challenge of Sustainability*.
- Fuchs, B.M., Woebken, D., Zubkov, M.V., Burkill, P., and Amann, R. (2005) Molecular identification of picoplankton populations in contrasting waters of the Arabian Sea. *Aquat Microb. Ecol.* 39:145–157
- Fuhrman, J.A. (1999) Marine viruses and their biogeochemical and ecological effects. *Nature*

399: 541–548.

- Galand, P.E., Potvin, M., Casamayor, E.O., and Lovejoy, C. (2010) Hydrography shapes bacterial biogeography of the deep Arctic Ocean. *ISME J.*, 4, 564–576.
- Giovannoni, S.J., Rappe, M.S., Vergin, K.L., and Adair, N.L. (1996) 16S rRNA genes reveal stratified open ocean bacterioplankton populations related to the Green Non-Sulfur bacteria. *Proc Natl Acad Sci USA* 93: 7979–7984.
- Giovannoni, S.J., and Stingl, U. (2005) Molecular diversity and ecology of microbial plankton. *Nature* 437:343–348.
- Gordon, D.A., and Giovannoni, S.J. (1996) Detection of stratified microbial populations related to *Chlorobium* and *Fibrobacter* species in the Atlantic and Pacific Oceans. *Appl. Environ. Microbiol.* 62:1171–1177.
- Hansell, D.A., and Ducklow, H.W. (2003) Bacterioplankton distribution and production in the bathypelagic ocean: Directly coupled to particulate organic carbon export?, *Limnol. Oceanogr.*, 48, 150–156.
- Handelsman, J. (2004) Metagenomics: application of genomics to uncultured microorganisms. *Microb. Molec. Biol. Rev.*, 68, 669–685.
- Helder, W., and de Vries, R. (1979) An automatic phenol- hypochlorite method for the detection of ammonia in sea- and brackish waters. *J. Sea Res.* 13: 154–160.
- Herndl, G.J., Reinthaler, T., Teira, E., van Aken, H., Veth, C., Pernthaler, A., and Pernthaler, J. (2005) Contribution of Archaea to total prokaryotic production in the deep Atlantic Ocean. *Appl. Environ. Microbiol.* 71, 2303–2309.
- Hugenholtz, P., Goebel, B.M., and Pace, N.R. (1998) Impact of culture- independent studies on the emerging phylogenetic view of bacterial diversity. *J. Bacteriol.* 180:4765–4774.
- Jannasch, H.W., and Jones, G.E. (1959) Bacterial populations in sea water as determined by different methods of enumeration. *Limnology and Oceanography* 4: 128-139.
- Karl, D.M. (2002) Nutrient dynamics in the deep blue sea. *Trend Microbio.* 10:410–418.
- Karner, M.B., De Long, E.F., and Karl, D.M. (2001) Archaeal dominance in the mesopelagic zone of the Pacific Ocean. *Nature* 409:507–510.
- Kirchman, D.L., Moran, X.A.G., and Ducklow, H. (2009) Microbial growth in the polar oceans – role of temperature and potential impact of climate change. *Nat Rev Microbiol* 7: 451–459.
- Larsson, U., and Hagström, A. (1979) Phytoplankton exudate release as an energy source for the growth of pelagic bacteria. *Mar. Biol.* 53. 199
- Lebaron, P., Parthuisot, N., and Catala, P. (1998) Comparison of blue nucleic acid dyes for flow cytometric enumeration of bacteria in aquatic systems. *Appl. Environ. Microbiol.* 64: 1725–1730.
- Longhurst, A.R. (1998) *Ecological geography of the sea*. Academic Press, San Diego, CA.

- Manz, W., Amann, R., Ludwig, W., Wagner, M., and Schleifer, K.H. (1992) Phylogenetic oligodeoxynucleotide probes for the major subclasses of Proteobacteria - problems and solutions. *Syst Appl Microbiol* 15:593–600
- Morris, R.M., Rappé, M.S., Connon, S.A., Vergin, K.L., Slebold, W.A., Carlson, C.A., and Giovanonni, S.J. (2002) SAR11 clade dominates ocean surface bacterioplankton communities. *Nature* 420: 806–810.
- Morris, R.M., Rappé, M.S., Urbach, E., Connon, S.A., and Giovanonni, S.J. (2004) Prevalence of the Chloroflexi-related SAR202 bacterioplankton cluster throughout the mesopelagic zone and deep ocean. *Appl. Environ. Microbiol.* 70: 2836–2842.
- Morris, R.M., Nunn, B.L., Frazar, C., Goodlett, D.R., Ting, Y.S., and Rocap, G. (2010) Comparative metaproteomics reveals ocean-scale shifts in microbial nutrient utilization and energy transduction. *ISME J.* 4: 673–685.
- Murphy, J. and Riley, J.P. (1962) A modified single solution method for the determination of phosphate in natural waters. *Anal. Chim. Acta* 27: 31–36.
- Nagata, T., Fukada, H., Fukuda, R., and Koike, I. (2000) Bacterioplankton distribution and production in deep Pacific waters: Large-scale geographic variations and possible coupling with sinking particle fluxes. *Limnol. Oceanogr.* 45: 426–435.
- Parsons, T., Maita, Y., and Lalli, Y. (1984) A manual of chemical and biological methods for seawater analysis. Pergamon Press.
- Patching, J. W., and Eardly, D. (1997) Bacterial biomass and activity in the deep waters of the eastern Atlantic—evidence of a barophilic community. *Deep-Sea Res. I* 44: 1655–1670.
- Pernthaler, A., Pernthaler, J., and Amann, R. (2004). Sensitive multi-color fluorescence in situ hybridization for the identification of environmental microorganisms. In: Kowalchuk GA, De Bruijn FJ, Head IM, Akkermans AD, van Elsas JD (eds). *Molecular Microbial Ecol* Man, 2nd edn. Kluwer Academic Publishers: Dordrecht, pp 711–726.
- Porter, K.G., and Feig, Y.S. (1980) The use of DAPI for identifying and counting aquatic microflora. *Limnol. Oceanogr.* 25:943–948.
- Reinthal, T., van Aken, H., Veth, C., Aristegui, J., et al. (2006) Prokaryotic respiration and production in the meso- and bathypelagic realm of the eastern and western North Atlantic basin. *Limnol Oceanogr* 51:1262–1273.
- Schattenhofer, M., Fuchs, B.M., Amann, R., Zubkov, M., Tarran, G.A., and Pernthaler, J. (2009) Latitudinal distribution of prokaryotic picoplankton populations in the Atlantic Ocean. *Environ. Microbiol.* 11:2078–2093.
- Simon, M., and Azam, F. (1989) Protein content and protein synthesis rates of planktonic marine bacteria. *Mar. Ecol. Prog. Ser.* 51: 201–213.
- Sogin, M.L., Morrison, H.G., Huber, J.A., et al. (2006) Microbial diversity in the deep sea and the underexplored “rare biosphere”. *Proc. Natl. Acad. Sci. U.S.A.* 103, 12115–12120.

- Sorokin, Y.I. (1981) Microheterotrophic organisms in marine ecosystems. In: Longhurst, A.R. (1998) Analysis of marine ecosystems. Academic Press, London, pp. 293–342.
- Stefels, J. (2000) Physiological aspects of the production and conversion of DMSP in marine algae and higher plants. *J Sea Res* 43: 183–197.
- Swan, B. K., Martinez-Garcia, M., Preston, C. M., Sczyrba, A., Woyke, T., Lamy, D., et al. (2011) Potential for chemolithoautotrophy among ubiquitous bacteria lineages in the dark ocean. *Science* 333, 1296–1300.
- Teira, E., Reinthaler, T., Pernthaler, A., Pernthaler, J., and Herndl, G.J. (2004) Combining catalyzed reporter deposition-fluorescence in situ hybridization and microautoradiography to detect substrate utilization by bacteria and Archaea in the deep ocean. *Appl Environ Microbiol* 70:4411–4414.
- Teira, E., Lebaron, P., Aken, H.M.V., Veth, C., and Herndl, G.J. (2006) Distribution and activity of Bacteria and Archaea in the deep water masses of the North Atlantic. *Limnol Oceanogr* 51: 2131–2144.
- van Aken, H.M. (2000) The hydrography of the mid-latitude northeast Atlantic Ocean: I. The deep water masses. *Deep-Sea Res. I* 47: 757–788.
- Varela, M.M., van Aken, H.M., and Herndl, G.J. (2008) Abundance and activity of Chloroflexi-type SAR202 bacterioplankton in the meso- and bathypelagic waters of the (sub)tropical Atlantic. *Environ. Microbiol.*, 10:1903–1911.
- Varela, M.M., van Aken, H.M., Sintes, E., Reinthaler, T., and Herndl, G.J. (2011) Contribution of Crenarchaeota and Bacteria to autotrophy in the North Atlantic interior. *Environ. Microbiol.*, 13(6), pp.1524–33.
- Warren, A.B., and Wunsch, C. (1981) Deep circulation of the world ocean. *Evol. Physic. Oceano.*, pages 6–40.
- Whitman, W.B, Coleman, D.C, and Wiebe, W.J (1998) Prokaryotes: The unseen majority. *Proc. Natl. Acad. Sci. USA* 95: 6578–6583.
- Woebken, D., Fuchs, B.M., Kuypers, M.M.M., and Amann, R. (2007) Potential interactions of particle-associated anammox Bacteria with bacterial and archaeal partners in the Namibian upwelling system. *Appl Environ Microbiol* 73: 4648–4657.
- Wuchter, C., Abbas, B., Coolen, M.J.L., Herfort, L., van Bleijswijk, J., Timmers, P., et al. (2006) Archaeal nitrification in the ocean. *Proc. Natl. Acad. Sci. USA*. 103: 12317–12322.
- Zehr, J.P., and Ward, B.B. (2002) Nitrogen cycling in the ocean: new perspectives on processes and paradigms. *Appl. Environ. Microbiol.* 68: 1015–1024.
- ZoBell, C.E., and Anderson, D.Q.(1936) Observations on the multiplication of bacteria in different volumes of sea water and the influence of oxygen tension and solid surfaces. *Biol. Bull. Woods Hole*. 71, 34–342.

7. Tables

Table 1. Physical and chemical characteristics of the major water masses of the oceanic provinces studied in the North Atlantic. Means and standard deviations are given for each water mass sampled. For abbreviations of oceanic provinces and water masses see Material and Methods.

Oceanic province	Water mass	Depth [m]	Salinity	Temperature [°C]	AOU [$\mu\text{mol L}^{-1}$]	NO ₃ [$\mu\text{mol L}^{-1}$]	PO ₄ [$\mu\text{mol L}^{-1}$]	Si [$\mu\text{mol L}^{-1}$]
NADR	100m	100 \pm 1	35.76 \pm 0.14	13.14 \pm 0.79	27.30 \pm 2.25	8.08 \pm 1.84	0.49 \pm 0.12	2.46 \pm 0.55
	O ₂ -min	794 \pm 258	35.48 \pm 0.34	9.54 \pm 1.00	98.14 \pm 3.23	18.25 \pm 1.27	1.13 \pm 0.11	9.53 \pm 0.64
	MSOW	1104 \pm 199	35.34 \pm 0.28	7.09 \pm 1.91	82.40 \pm 10.66	18.10 \pm 0.30	1.15 \pm 0.04	10.51 \pm 0.49
	AAIW	1531 \pm 253	35.03 \pm 0.07	4.57 \pm 0.53	65.30 \pm 6.12	17.94 \pm 0.18	1.16 \pm 0.01	11.18 \pm 0.76
	NADW	2749 \pm 3	34.94 \pm 0.01	3.05 \pm 0.10	72.88 \pm 4.29	18.15 \pm 0.50	1.20 \pm 0.03	19.46 \pm 2.75
	LDW	4039 \pm 58	34.92 \pm 0.00	2.59 \pm 0.02	103.00 \pm 0.94	22.08 \pm 0.23	1.48 \pm 0.01	41.67 \pm 0.77
NASR	100m	96 \pm 8	36.36 \pm 0.29	17.12 \pm 1.95	16.97 \pm 11.54	2.02 \pm 1.98	0.12 \pm 0.12	1.07 \pm 0.40
	O ₂ -min	702 \pm 89	35.58 \pm 0.10	10.76 \pm 0.63	89.53 \pm 16.65	16.88 \pm 2.22	1.02 \pm 0.14	7.85 \pm 1.96
	MSOW	1000 \pm 101	35.65 \pm 0.17	9.20 \pm 1.41	96.33 \pm 3.87	18.27 \pm 1.24	1.12 \pm 0.10	10.55 \pm 1.65
	AAIW	1533 \pm 58	35.19 \pm 0.12	5.30 \pm 0.80	74.43 \pm 5.09	18.21 \pm 0.07	1.15 \pm 0.01	12.04 \pm 0.39
	NADW	2750 \pm 1	34.95 \pm 0.01	2.94 \pm 0.12	84.37 \pm 3.93	19.62 \pm 0.58	1.29 \pm 0.04	26.44 \pm 3.56
	LDW	4170 \pm 60	34.91 \pm 0.00	2.53 \pm 0.03	102.07 \pm 0.78	22.29 \pm 0.13	1.48 \pm 0.01	42.76 \pm 0.71
NATR	100m	100 \pm 1	36.90 \pm 0.27	20.38 \pm 1.25	-0.33 \pm 3.95	0.01 \pm 0.01	0.01 \pm 0.00	0.61 \pm 0.10
	O ₂ -min	826 \pm 24	35.37 \pm 0.12	9.28 \pm 0.78	119.59 \pm 13.94	21.66 \pm 2.48	1.34 \pm 0.17	12.10 \pm 2.36
	MSOW	1133 \pm 118	35.30 \pm 0.16	7.13 \pm 1.18	109.71 \pm 5.74	21.63 \pm 1.57	1.37 \pm 0.12	14.63 \pm 2.36
	AAIW	1693 \pm 12	35.14 \pm 0.03	4.84 \pm 0.17	86.55 \pm 6.96	19.71 \pm 0.95	1.27 \pm 0.07	16.45 \pm 1.60
	NADW	2747 \pm 1	34.96 \pm 0.00	2.94 \pm 0.03	92.79 \pm 4.59	20.73 \pm 0.63	1.38 \pm 0.05	30.54 \pm 1.97
	LDW	4701 \pm 265	34.90 \pm 0.01	2.44 \pm 0.06	102.85 \pm 0.49	22.58 \pm 0.22	1.50 \pm 0.01	45.55 \pm 1.58

Table 2. Biological characteristics of the major water masses in the oceanic provinces of the North Atlantic. Prokaryotic abundance (PA), high nucleic acid containing prokaryotes (HNA). Means and standard deviations are given for each water mass sampled. For abbreviations of oceanic provinces and water masses see Material and Methods.

Oceanic Province	Water mass	PA [10 ⁵ mL ⁻¹]	HNA [%]	Leu incorporation [pmol L ⁻¹ d ⁻¹]	Production cell ⁻¹ [amol C cell ⁻¹ d ⁻¹]
NADR	100m	3.73 ± 0.81	55.44 ± 1.51	25.66 ± 4.81	17.76 ± 5.09
	O ₂ -min	0.84 ± 0.36	60.00 ± 1.19	2.63 ± 1.25	8.11 ± 5.20
	MSOW	0.54 ± 0.11	59.63 ± 4.56	1.42 ± 0.65	6.82 ± 3.42
	AAIW	0.39 ± 0.02	62.75 ± 6.49	0.62 ± 0.29	4.06 ± 1.92
	NADW	0.26 ± 0.06	63.47 ± 6.61	0.25 ± 0.06	2.45 ± 0.86
	LDW	0.29 ± 0.04	68.32 ± 6.44	0.35 ± 0.21	3.16 ± 1.89
NASR	100m	3.23 ± 0.75	44.88 ± 5.91	52.02 ± 34.29	41.56 ± 29.03
	O ₂ -min	0.56 ± 0.23	49.28 ± 2.63	1.98 ± 1.63	9.21 ± 8.49
	MSOW	0.39 ± 0.12	54.95 ± 1.06	0.94 ± 0.16	6.25 ± 2.15
	AAIW	0.22 ± 0.08	53.58 ± 5.56	0.28 ± 0.05	3.24 ± 1.25
	NADW	0.15 ± 0.02	57.06 ± 5.63	0.14 ± 0.02	2.43 ± 0.52
	LDW	0.11 ± 0.02	62.78 ± 2.02	0.09 ± 0.03	2.13 ± 0.79
NATR	100m	4.33 ± 0.17	39.12 ± 4.70	168.69 ± 68.37	100.63 ± 40.97
	O ₂ -min	0.38 ± 0.06	55.19 ± 2.47	0.51 ± 0.22	3.52 ± 1.60
	MSOW	0.30 ± 0.11	55.15 ± 9.95	0.27 ± 0.21	2.30 ± 1.96
	AAIW	0.22 ± 0.06	58.10 ± 12.53	0.13 ± 0.08	1.57 ± 1.03
	NADW	0.11 ± 0.02	59.29 ± 2.65	0.06 ± 0.01	1.40 ± 0.36
	LDW	0.10 ± 0.04	62.05 ± 3.47	0.04 ± 0.00	0.89 ± 0.39

able 3. Spearman rank correlation of the relative abundances of Bacteria, SAR11, SAR324, SAR202, Crenarchaeota (Cren) and Euryarchaeota (Eury) and the cell-specific production of Bacteria (BP cell⁻¹ d⁻¹) and of Crenarchaeota (CRP cell⁻¹ d⁻¹) with the biogeochemical variables of the North Atlantic. For abbreviations of the biogeochemical variables see Material and Methods.

Parameter	Bacteria	SAR11	SAR324	SAR202	Cren	Eury	BP cell ⁻¹	CRP cell ⁻¹
Salinity	0.592 **	0.080	- 0.388	- 0.592 **	0.349	- 0.242	0.392	0.205
Temperature	0.562 *	0.102	- 0.414	- 0.658 **	0.423	- 0.238	0.367	0.226
AOU	- 0.516 *	- 0.524 *	0.422	0.494 *	- 0.249	0.429	- 0.419	- 0.261
Nitrate	- 0.704 **	- 0.414	0.549 *	0.619 **	- 0.315	0.468 *	- 0.448	- 0.263
PA	0.655 **	0.100	- 0.663 **	- 0.657 **	0.489	- 0.406	0.418	0.418
HNA	0.660 **	0.143	- 0.702 **	- 0.661 **	0.550	- 0.450	0.396	0.472 *
Leu incorporation	0.704 **	0.056	- 0.715 **	- 0.697 **	0.438	- 0.462	0.448	0.459
Production cell ⁻¹ d ⁻¹	0.754 **	0.089	- 0.718 **	- 0.742 **	0.382	- 0.495 *	0.490 *	0.478 *

* p < 0.05

** p < 0.01

9. Figures

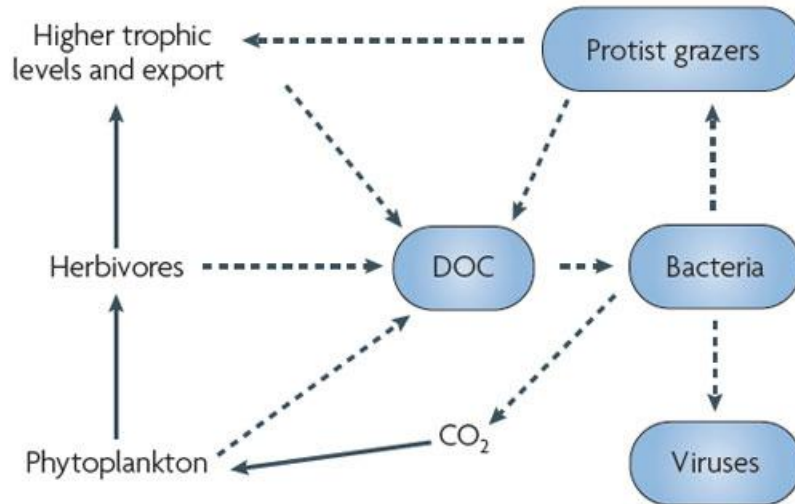


Figure 1. Simplified scheme of the microbial loop as originally proposed by Azam et al. (1983) redrawn from Kirchman et al. (2009). Phytoplankton include cyanobacteria as major components of the phytoplankton community in some oceans. The loop refers to losses of dissolved organic carbon (DOC) from all organisms and its utilization in the food web by heterotrophic bacteria. Solid arrows represent trophic linkages before the introduction of the microbial loop by Azam et al. (1983). Broken arrows represent trophic linkages summarized as the microbial loop.

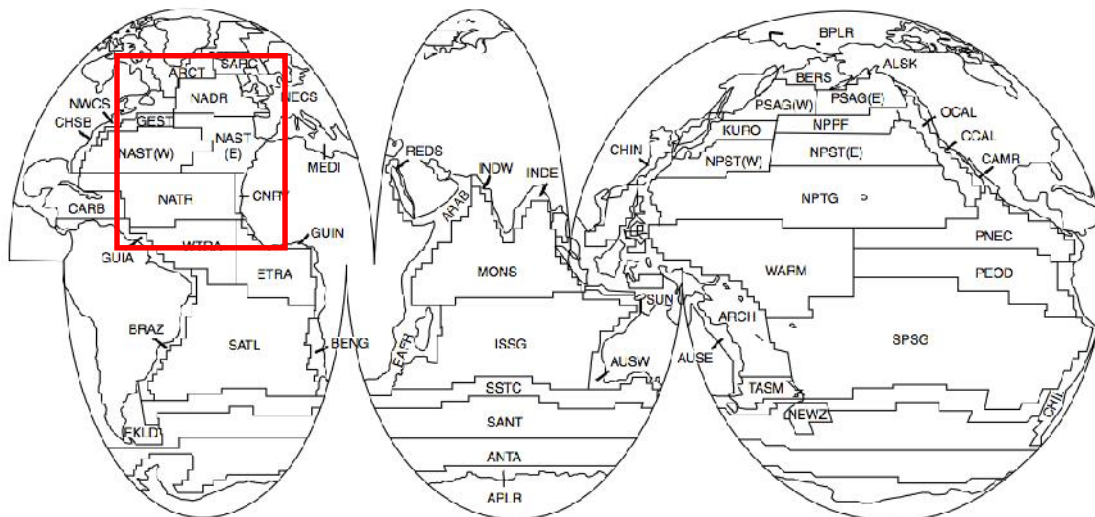


Figure 2. Classification scheme of biogeographical provinces by Longhurst (1998). The oceanic provinces according to Longhurst indicate areas with typical characteristics in turbulence, temperature, irradiance and nutrients and thus, form four principal biomes that can be found in the major oceans: the polar biome, the westerlies biome, the trade-wind biome and the coastal boundary-zone biome. Highlighted by the red box is the sampling area of this study in the North Atlantic Ocean.

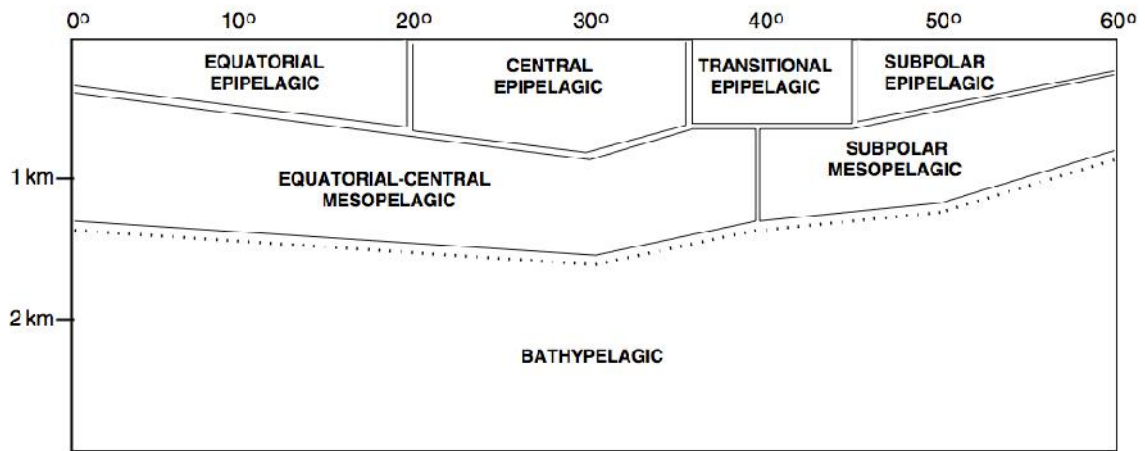


Figure 3. Proposed scheme of Brinton (1962) classifying the ocean into four epipelagic provinces, two mesopelagic provinces and one homogeneous bathypelagic province. The scheme of Brinton is based on the distribution of groups of pelagic species with latitude and depth along a meridional section in an idealized ocean.

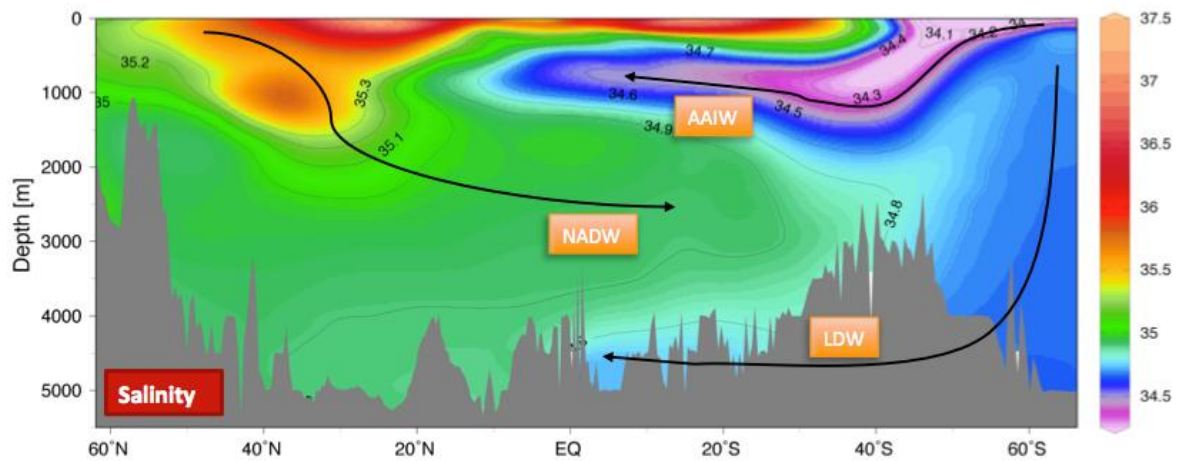


Figure 4. Distribution of salinity and water-mass transport through the Atlantic Ocean. The main water masses are shown; Lower Deep Water (LDW), the North Atlantic Deep Water (NADW) and the Antarctic Intermediate Water (AAIW).

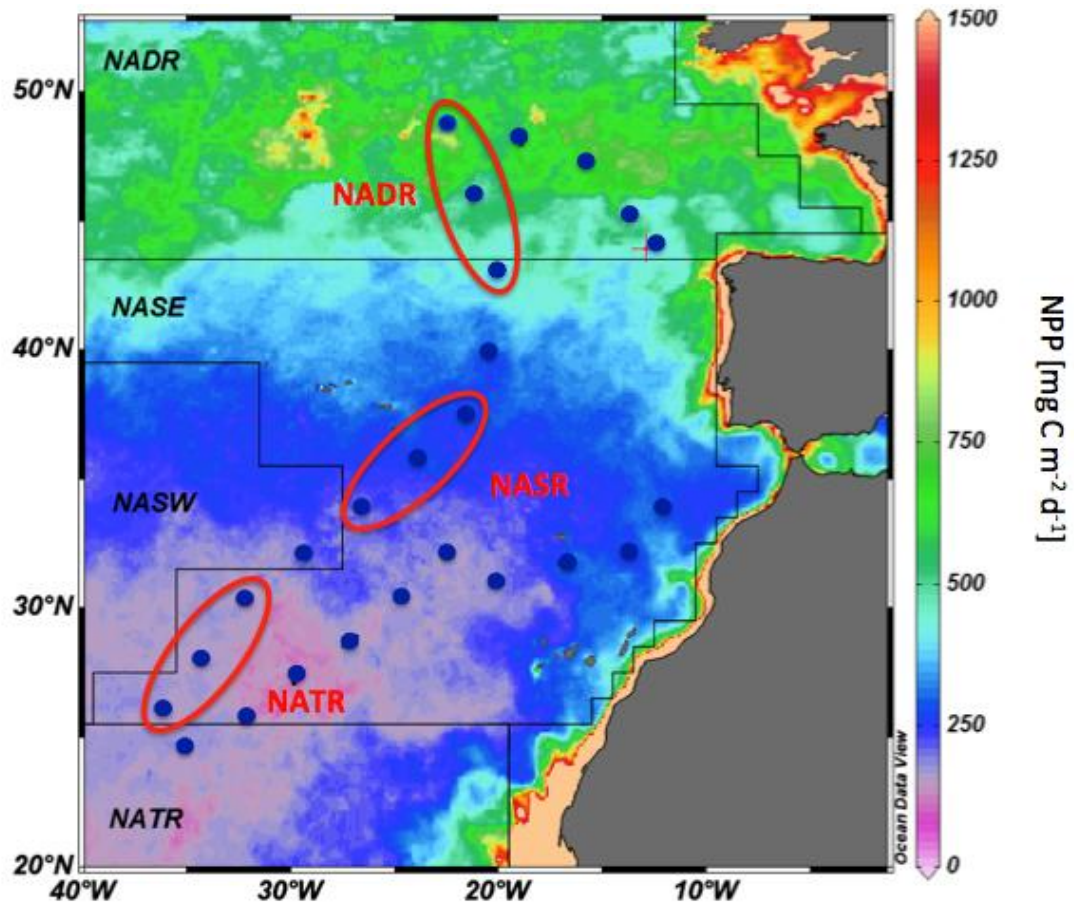


Figure 5. Map of the cruise track and stations occupied during the MEDEA 1 expedition. The net primary production (NPP) (given in $\text{mg C m}^{-2} \text{d}^{-1}$) was retrieved from the ocean productivity website www.science.oregonstate.edu/ocean.productivity/ for the weeks were the expedition took place (Oct-Nov 2011). Black lines demark the borders of the standard Longhurst provinces (Longhurst 1998). The red ellipses indicate the analyzed stations in the different oceanic provinces. Stations are indicated by blue dots. The provinces determined and arranged according to NPP rates during the expedition MEDEA 1 along the transect are the North Atlantic Drift Region (NADR), the North Atlantic Subtropical Region (NASR) and the North Atlantic Tropical Region (NATR).

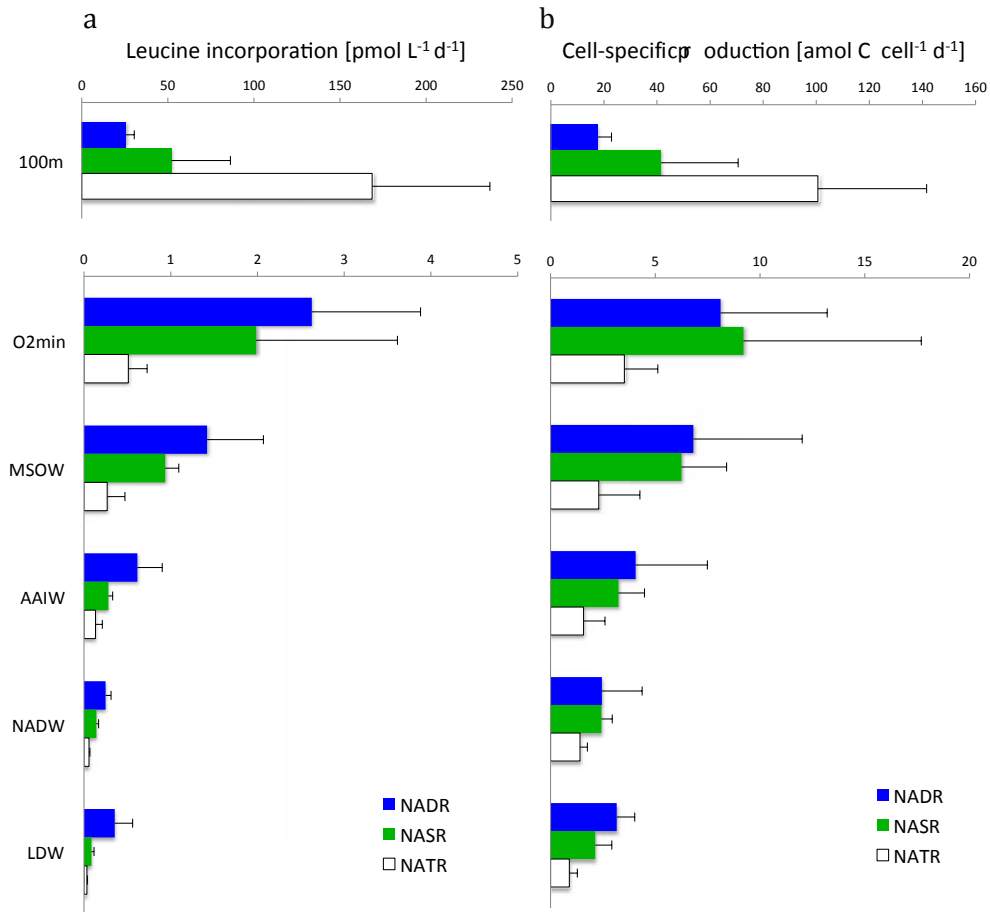


Figure 6. Leucine incorporation of the bulk prokaryotic community ($\text{pmol L}^{-1} \text{d}^{-1}$) **(a)** and cell-specific production ($\text{amol C cell}^{-1} \text{d}^{-1}$) **(b)** in the different water masses and grouped according to the oceanic provinces along the transect. Colored bars represent the averages ($n = 3$) of stations sampled. Error bars indicate standard deviations. For abbreviations of water masses and provinces see Material and Methods.

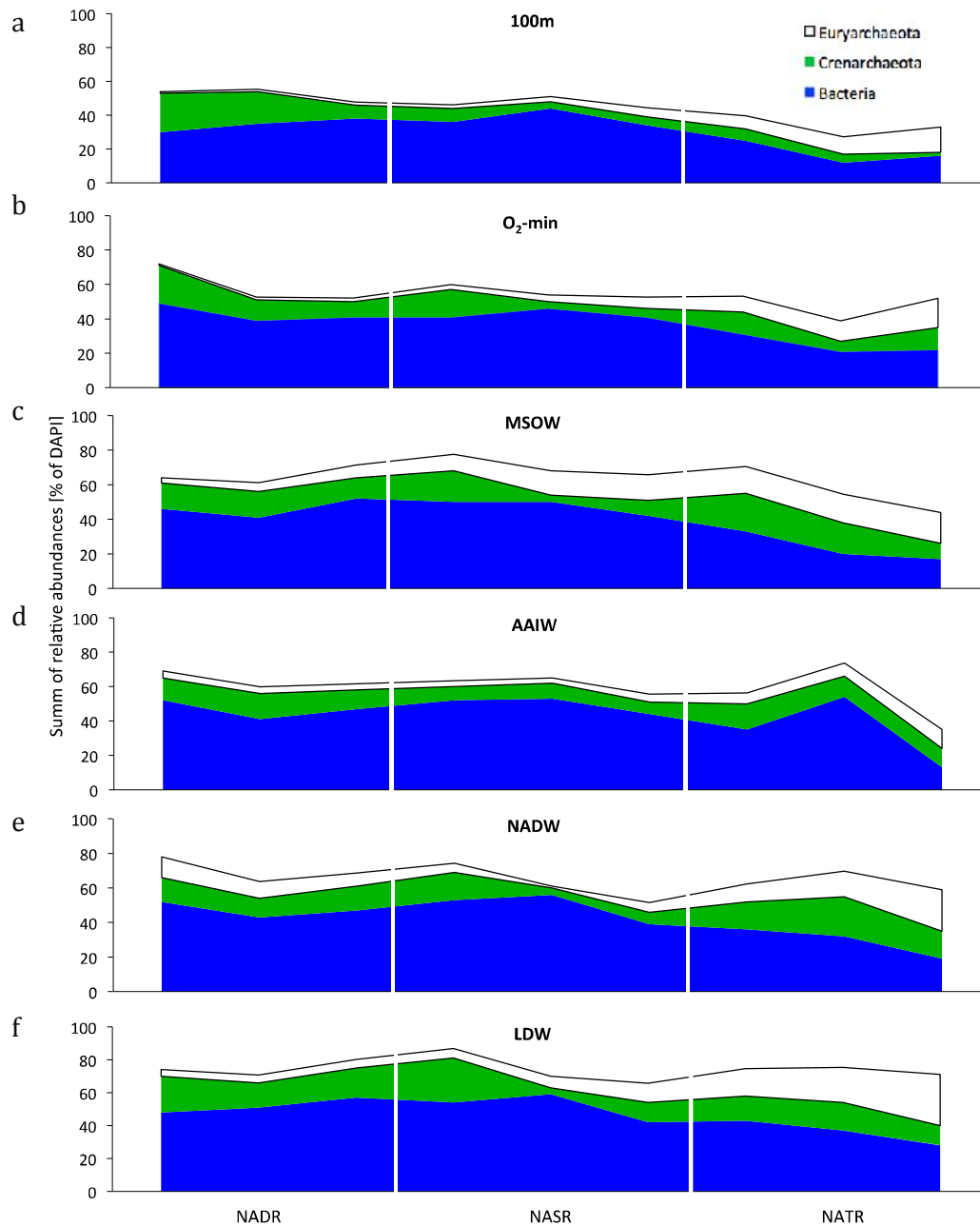


Figure 7. Relative contribution of Bacteria, Crenarchaeota and Euryarchaeota along the nine stations of the transect separated in oceanic provinces (Longhurst, 1998). Values indicate averages of the relative abundances based on DAPI cell counts in the 100 meter depth layer (**a**), oxygen minimum layer (O₂-min) (**b**), Mediterranean Sea Outflow Water (MSOW) (**d**), Antarctic Intermediate Water (AAIW) (**d**), North Atlantic Deep Water (NADW) (**e**), Lower Deep Water (LDW) (**f**). For abbreviations of the oceanic provinces and water masses see Material and Methods.

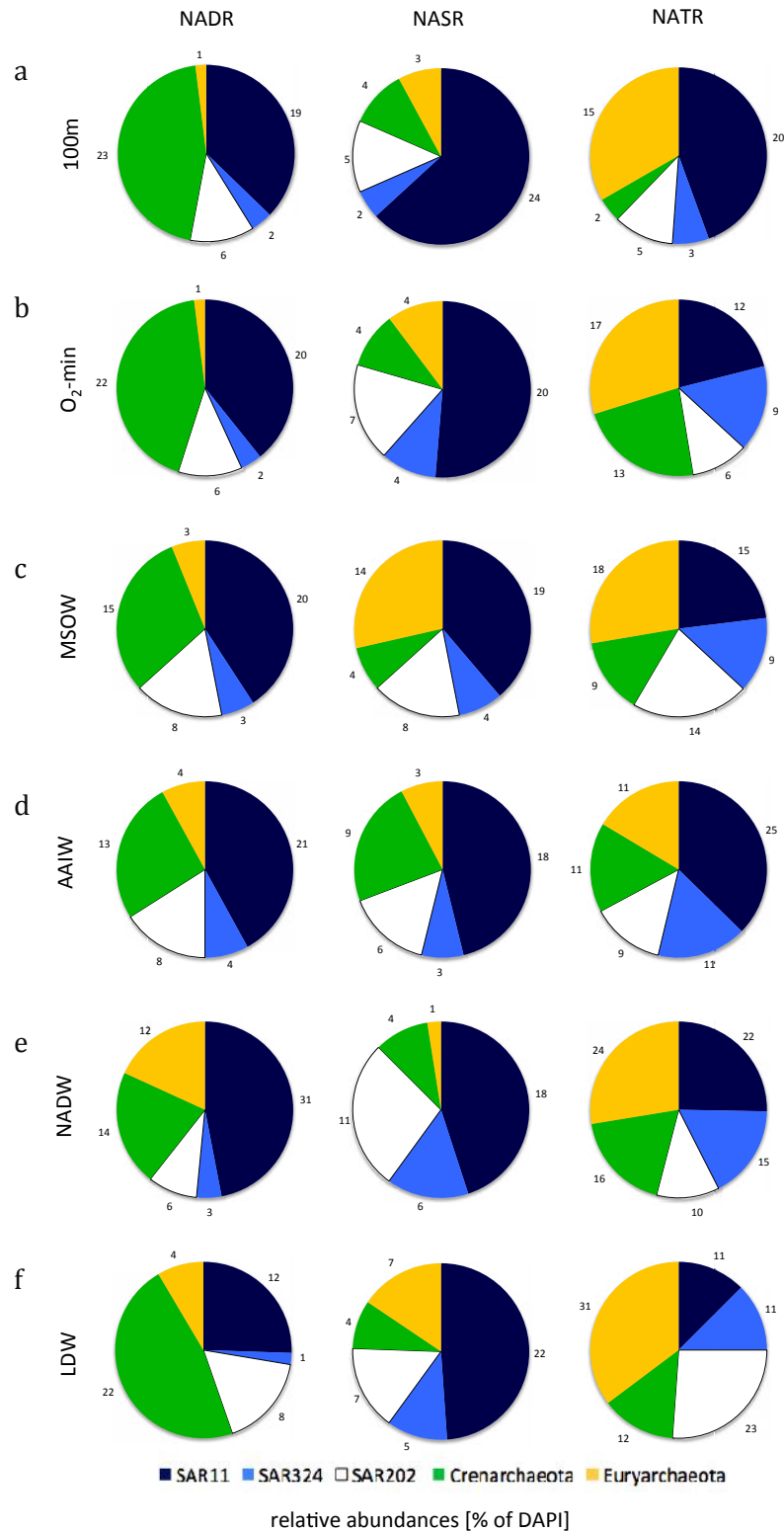


Figure 8. Contribution of the major prokaryotic groups in the different water masses according to the oceanic provinces (Longhurst, 1998). Numbers indicate relative abundances in percent of DAPI cell counts in the 100 meter depth layer (a), the oxygen minimum layer (O₂-min) (b), Mediterranean Sea Outflow Water (MSOW) (c), Antarctic Intermediate Water (AAIW) (d), North Atlantic Deep Water (NADW) (e), Lower Deep Water (LDW) (f). For abbreviations of oceanic provinces and water masses see Material and Methods.

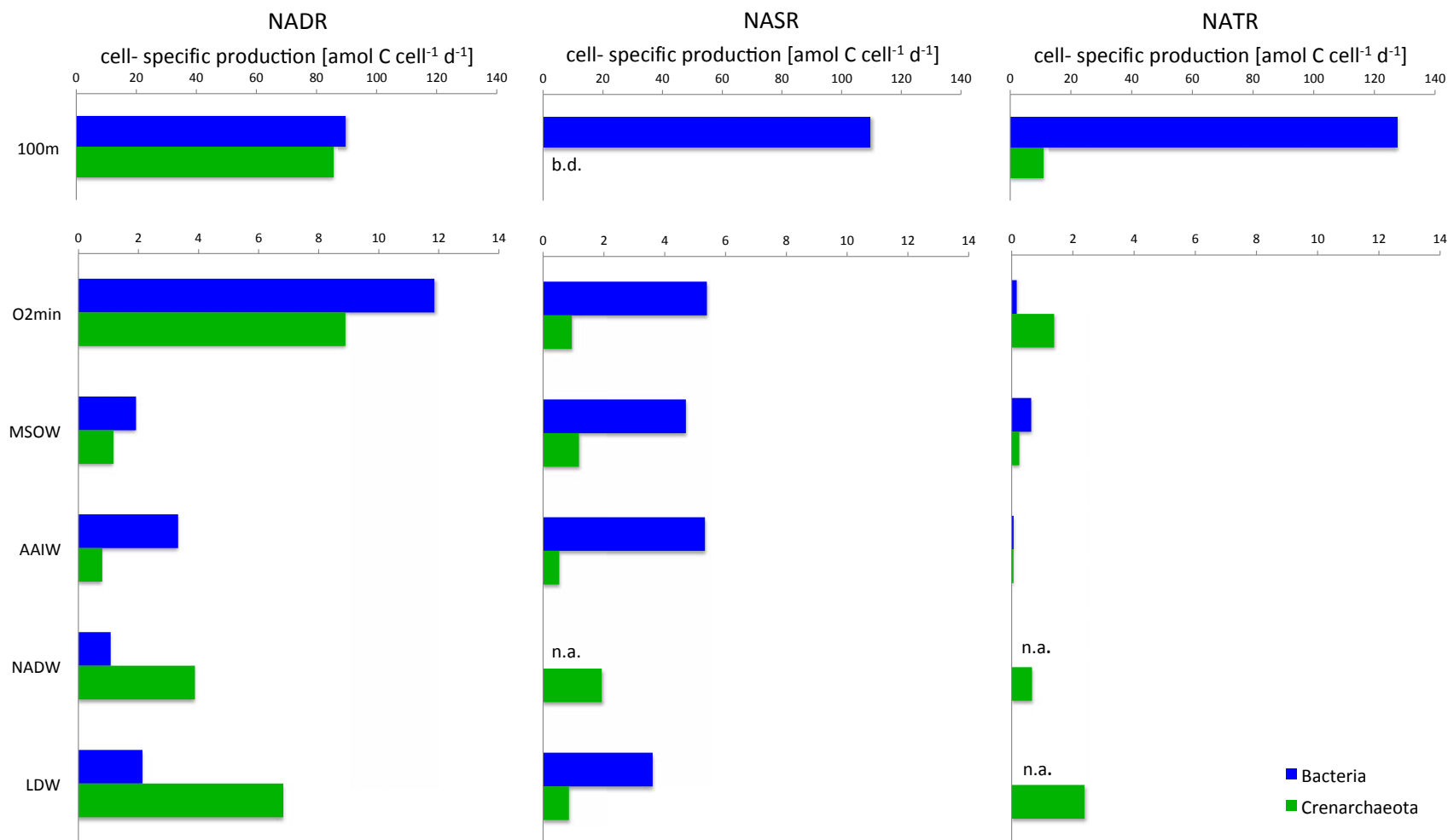


Figure 9. Mean cell-specific production of Bacteria and Crenarchaeota in the different water masses of the three oceanic provinces NADR, NASR and NATR. For abbreviations of water masses and oceanic provinces see Material and Methods. Bad data quality (b.d.) and no detectable activity (n.a.) are indicated.

10. Supplementary Information

10.1. CARD-FISH and Micro-CARD-FISH protocols

10.1.1. Catalyzed reporter deposition fluorescence in situ hybridization (CARD-FISH)

The relative abundance of Bacteria and Archaea for all stations along the transect occupied during the MEDEA 1 cruise in the North Atlantic was determined using catalyzed reporter deposition fluorescence in situ hybridization (CARD-FISH). The relative abundance of the bacterial subgroups SAR11, SAR406, SAR324 and SAR202 and the archaeal divisions Crenarchaeota and Euryarchaeota were enumerated for the most northern, the central and the most southern stations along the transect. The relative activity of Bacteria and Crenarchaeota was determined for station 5, station 7, station 10, station 11, station 12 and station 15, using microautoradiography catalyzed reporter deposition fluorescence in situ hybridization (Micro-CARD-FISH).

Sampling and Sample Fixation

The water samples from the distinct water layers and water masses were collected in acid cleaned (0.1M) and three times Milli-Q washed polycarbonate bottles directly from the Niskin bottles. Immediately after collecting the water, samples were fixed by adding filtered paraformaldehyde [37%] to a final concentration of 2%.

Depending on the depth layer, different volumes of duplicate seawater samples were fixed in Greiner tubes (Greiner bio one). For the LDW, 80mL, for NADW and AAIW 40 mL, for the MSOW 30mL and for the O₂-min and 100m layers 20mL of sample water were fixed and allowed to sit in the dark at 4°C for 18h.

Thereafter, the fixed water samples were filtered through a 0.2-mm pore size polycarbonate filter (Millipore, GTTP, 25-mm diameter) supported by a 0.45mm pore size cellulose nitrate filter (Millipore, HAWP, 25-mm diameter). After the filtration, each filter was washed with 5-10 mL of fresh Milli-Q water, air-dried and stored in a Microfuge tube at -20°C until further processing in the home laboratory. For each depth duplicates were processed.

Embedding

In the home laboratory, the CARD-FISH filters were thawed to room temperature and embedded cell side down into a drop of 0.1% low melting point agarose in a petri dish (sea plaque GTGagarose, FMC bioProducts) and dried in a hybridization oven at 37°C for 15 min. After drying, the filters were detached using 95% ethanol and briefly dried on blotting paper.

Only half a filter was embedded to minimize the risk of loosing samples during the embedding process. The filters were embedded with care to avoid contact of the cell side (the side where the cells have been filtered onto) of the filter with the bottom of the petri dish to prevent cell loss. Moreover, the filters were only touched with forceps at the 3mm rim around the filter. Forceps and scissors were cleaned with 95% ethanol before use.

The dried filters were cut with scissors into small sections and labelled according to station, depth and target probe with a 0.3mm retractable pencil at the outer filter edges. Filter sections not directly processed further were stored in Microfuge tubes in the dark at -20°C.

Permeabilization

The filter sections for targeting Bacteria, the bacterial cluster SAR11, the bacterial clade SAR406, the bacterial clade SAR324 and the bacterial cluster SAR202 were incubated in a permeabilization buffer containing white lysozyme from chicken egg (50,000 Units mg^{-1} , Sigma-Aldrich), see Table below. The filter sections targeting Crenarchaeota and Euryarchaeota were incubated in a permeabilization buffer containing proteinase-K from Tritirachium album (>800 Units mL^{-1} , Sigma-Aldrich), see Table below. The permeabilization buffer was prepared in 15mL Greiner tubes and contained Tris-HCl [1M], EDTA [0.5M] and fresh Milli-Q water, for concentrations see table below and for exact name and company the chemical supply list.

The solution was vortexed until precipitates had dissolved. The filter sections were put into the Greiner tube, agitated until filter sections were covered with solution and thereafter, incubated in an hybridization oven at 37°C with the lid open for 1 h.

Permeabilization buffer for Lysozyme:

Stock reagent	Volume	Final concentration
Lysozyme	100mg	10mg/mL
Tris-HCl [1M]	1000 μ L	0.1M
EDTA [0.5M]	1000 μ L	0.05M
Milli-Q water	fill up to 10mL	

Permeabilization buffer for Proteinase-K:

Stock reagent	Volume	Final concentration
Proteinase-K	5 μ L	10.9mg/mL
Tris-HCl [1M]	1000 μ L	0.1M
EDTA [0.5M]	1000 μ L	0.05M
Milli-Q water	fill up to 10mL	

Subsequently, the solution containing the filter sections was poured in a Buechner funnel and filters were washed once to three times carefully with fresh Milli-Q water, once for lysozyme and three times for the proteinase-K treatment. Then, filter sections were placed in a HCl [0.01M] bath in a petri dish at room temperature for 25 min, then washed twice in the Buechner funnel with fresh Milli-Q water, rinsed with 95% ethanol and finally placed with the cell side up on a plotting paper to air-dry.

Hybridization

The following hybridization step was either performed directly after the permeabilization, or after storing the filter sections in microfuge tubes in the dark at -20°C for a maximum of 1 week.

Different horseradish peroxidase (HRP) oligonucleotide probes or probe-mixes were used during the hybridization step to target either Bacteria, the bacterial cluster SAR11, the bacterial clade SAR406, the bacterial clade SAR324, the bacterial cluster SAR202, Crenarchaeota and Euryarchaeota, see Table HRP probes. In addition to target the relative abundance of the bacterial clade SAR324, a helper was used (an oligonucleotide probe without HRP at the 5' end -see chapter HRP probes).

For the hybridization, 15 μ L of each probe was transferred into a 1.5 mL microfuge tube and the tube filled up to 300 μ L with the specific hybridization buffer, see chapter preparation before lab work. Probes were added to hybridization buffer at a volume ratio of 1:20 for each probe.

For the hybridization, the filter sections were piled up neatly and put into the corresponding tube containing the hybridization mix. The tubes were wrapped with aluminum foil to prevent exposure to light, mounted on the rotating pole of the hybridization oven and incubated under slow rotation at 35°C for 17 h. The hybridization process was terminated by transferring the filter sections into the pre-warmed (37°C) washing buffer.

For the hybridization to target **Bacteria**, 255 μ L of the 55%-formamide containing hybridization buffer was pipetted into an 1.5mL microfuge tube and 15 μ L of the one-fold concentrated EUB338 I probe (Amann et al., 1990), 15 μ L of the one-fold concentrated EUB338 II probe (Daims et al., 1999) and 15 μ L of the one-fold concentrated EUB338 III probe (Daims et al., 1999) was added to the microfuge tube and briefly vortexed.

For the hybridization to target the bacterial cluster **SAR11**, 240 μ L of the 45%-formamide containing hybridization buffer was pipetted into an 1.5mL microfuge tube and 15 μ L of the one-fold concentrated SAR11-152R probe (Morris et al., 2002), 15 μ L of the one-fold concentrated SAR11-441R probe (Morris et al., 2002), 15 μ L of the one-fold concentrated SAR11-542R probe (Morris et al., 2002) and 15 μ L of the one-fold concentrated SAR11-732R probe (Morris et al., 2002) was added and briefly vortexed.

For the hybridization to target the bacterial clade **SAR406**, 285 μ L of the 65%-formamide containing hybridization buffer was pipetted into an 1.5mL microfuge tube and 15 μ L of the one-fold concentrated SAR406-97 probe (Fuchs et al., 2005) was added and briefly vortexed. Despite similar hybridization conditions our higher formamide concentration should compensate the higher temperatures used in other studies (Schattenhofer et al., 2009; Allers et al., 20013), unspecific binding of the probe might have resulted in a higher abundance of SAR406 targeted bacteria.

Consequently, the date of the SAR406 targeted MGA bacteria were not analyzed in this study due to questionable date quality

For the hybridization to target the bacterial clade **SAR324**, 270 μ L of the 35%-formamide containing hybridization buffer was pipetted into an 1.5mL microfuge tube and 15 μ L of the one-fold concentrated SAR324-625 probe (Fuchs et al., 2005) and 15 μ L of the one-fold concentrated helper (Fuchs et al., in prep.) was added and briefly vortexed.

For the hybridization to target the bacterial cluster **SAR202**, 270 μ L of the 35%-formamide containing hybridization buffer was pipetted into an 1.5mL microfuge tube and 15 μ L of the one-fold concentrated SAR202-102R probe (Morris et al., 2004) and 15 μ L of the one-fold concentrated SAR202-312R (Morris et al., 2004) was added to the tube and briefly vortexed.

For the hybridization to target the **Crenarchaea**, 270 μ L of the 20%-formamide containing hybridization buffer was pipetted into an 1.5mL microfuge tube and 15 μ L of the one-fold concentrated CREN537 probe (Teira et al., 2004) and 1.5mL microfuge tube and 15 μ L of the one-fold concentrated CREN554 probe (Woebken et al., 2007) was added and briefly vortexed.

For the hybridization to target the **Euryarchaea**, 285 μ L of the 20%-formamide containing hybridization buffer was pipetted into an 1.5mL microfuge tube and 15 μ L of the one-fold concentrated EURY806 probe (Teira et al. 2004) was added to the tube and briefly vortexed.

For the hybridization with the **NonEUB** probe, 285 μ L of the 55%-formamide containing hybridization buffer was pipetted into an 1.5mL microfuge tube and 15 μ L of the one-fold concentrated Non338 probe (Manz et al., 1992) was added and briefly vortexed.

Washing and PBS-T-mix

The washing buffer was mixed in a 50mL Greiner tube and prepared individually for each probe mix with the appropriate formamide concentration of the hybridization buffer used. The washing buffer contained a variable amount of NaCl [5M], depending on the formamide concentration of the hybridization buffer (see table), and Tris-HCl [1M], EDTA [0.5M], fresh Milli-Q water and SDS [10%] (for concentrations see table below and for names and companies the chemical supply

list). After adding NaCl, Tris-HCl and EDTA, the tube was filled up with fresh Milli-Q water to 50mL and to avoid excessive bubble formation, the SDS was added last.

Washing buffer NaCl [5M] concentrations:

Formamide concentration Hybridization buffer	Amount of NaCl [5M] added to Washing Buffer
20%	1350 μ L
35%	420 μ L
45%	160 μ L
55%	30 μ L
65%	0 μ L

Washing buffer chemicals

Stock reagent	Volume	Final concentration
NaCl [5M]	see table above	
Tris-HCl [1M]	1000 μ L	20mM
EDTA [0.5M]	500 μ L	5mM
Milli-Q water	fill up to 49950 μ L	
SDS [10%]	50 μ L	0.01%

The washing buffer was pre-warmed to 37°C in the water bath or hybridization oven before filter sections were directly transferred into solution. Then, the washing buffer was briefly shaken until all filter sections were randomly distributed in the solution, and left in the hybridization oven at 35°C for 15 min.

Meanwhile the PBS-T-Mix was prepared in a 50mL Greiner tube, containing 49,975 μ L PBS [1x] and 25 μ L of TritonTM X-100 [100%], for detailed information about chemicals see list. The solution was well mixed until no phases could be seen and stored temporarily in the dark at room temperature.

After the washing process, the washing buffer containing the filter sections was poured in the Buechner funnel. The filter sections were put in a petri dish containing 25mL of the PBS-T-Mix prepared before and incubated in the solution in the dark for 15 min.

Amplification

In the meantime the amplification mix was prepared consisting of the amplification buffer, (see chemicals prepared before lab work) the tyramide dye Alexa Fluor 488 and H₂O₂ [30%] (for

detailed information about chemicals see list). For the preparation of the amplification 200 μ L and 493 μ L of the amplification buffer was transferred into 1.5mL microfuge tubes, each chemical in a separate tube. The following steps were performed in dimmed light conditions and on ice to avoid damage and modification of the chemicals.

Into the microfuge tube “A” containing 200 μ L amplification buffer, 1 μ L of H₂O₂ [30%] was added, briefly vortexed and immediately placed back on ice. To the microfuge tube “B”, containing 493 μ L amplification buffer, 5 μ L of the tyramide dye Alexa488 and 5 μ L of the solution of EPPi “A” were added and briefly vortexed.

The filter sections were piled up neatly directly after the incubation in the PBS-T-Mix and transferred into the Microfuge tube “B” containing the amplification mix. The tube was wrapped with aluminum foil, fixed to the rotor pole in the hybridization oven and incubated under slow rotation at 37°C for 45 min.

After the amplification, the filter sections were placed with the cell side up on plotting paper and air-dried. The dry filter sections were then put into the Greiner tube holding the remaining 25mL PBS-T-Mix and incubated in the dark at room temperature for 10 min before the filter sections were placed on plotting paper air-drying.

DAPI staining

The dried filter sections were placed with the cell side up onto slides which have been placed on ice. Each filter was inoculated with 50 μ L of freshly prepared DAPI-MQ-Mix (recipe see preparations before lab work) and incubated for 3 min.

Afterwards the filter sections were briefly dipped in EtOH [80%] to leach out the excessive DAPI and to reduce the signal-noise of the background. Then, the filter sections were rinsed with fresh Milli-Q water and placed on plotting paper and air-dried.

Finally the filter sections were transferred onto glass slides and mounted in a Vectashield-Citifluor-Mix, to avoid bleaching of the signal. The slides were then stored at -20°C in the dark.

10.1.2. Microautoradiography catalyzed reporter deposition fluorescence in situ hybridization (Micro-CARD-FISH)

Before starting the Micro-CARD-FISH protocol, the diluted photographic emulsion (Autoradiography Emulsion Type NTB-2, Kodak), for details see chemical list, was melted in the dark in a water bath set at 45°C for around 30 min. Moreover, the workplace in the dark room was arranged to facilitate the following work steps performed in the dark with a night vision device. The workplace provided the melted photographic emulsion in the water bath, a pair of forceps, aluminum foil, and clean slides, kimwipes to clean the bottom of the slides dipped into the photographic emulsion, and an ice-box containing ice with a aluminum plate on top to cool and dry the slides tipped into the emulsion, rubber foam coated carrier slides holding the hybridized filter sections, and a light-tight slide box for the exposure containing fresh silica gels in the lid as a drying agent.

The subsequently described working steps were performed in total darkness with a night vision device and an infrared light. The infrared light lamp was further blocked with black tape to reduce the emitted light. Additionally, the effects of the direct influence of the infrared light on the photographic emulsion was tested by analyzing slides covered with emulsion once using the night vision device and once performed in total darkness, showing no differences between the two treatments.

Embedding and Exposure

The empty slides were dipped on both sides into the vial holding the photographic emulsion until the whole slide surface was coated with emulsion. The bottom of the slide was then cleaned with kimwipes and the slides were placed onto the ice-cold aluminum plate to dry for 5 min.

The previously hybridized filter sections were transferred with the cell side up onto the rubber foam coated carrier slides. The filter sections were fixed to the rubber foam by a small droplet of water. Subsequently, the filter sections were stamped upside down into the emulsion onto the photographic emulsion coated slides. The slides were then placed cell side up in the light-tight slide box. The box was additionally wrapped twice in aluminum foil and kept at 4°C for

exposure. The exposure time varied between the water layer 100m and the deeper layers O₂-min, MSOW, AAIW, NADW and LDW. The 100m water samples were exposed for 3 d and the deeper water samples were exposed for 7d. The influence of the exposure time on the percentage of cells taking up L-[³H]Asp was evaluated with water samples from a test station and all depths.

Development

After the exposure, the slides were developed and fixed in total darkness under the night vision device using the KODAK developer and KODAK fixer (preparation see chapter preparations before lab work) and for detailed information about chemicals see chemical list. Prior to the developing and fixing step, the slides were pre-warmed to room temperature for 1h. The slides were then developed in the developer for 2 min. To stop the developing process, the slides were transferred afterwards into a fresh Milli-Q water bath for 10sec, then fixed in fixer for 5min and finally put into a new fresh Milli-Q water bath for at least 2 min.

The developed slides were transferred and further processed under day-light conditions. The slides were placed cell side up to dry onto paper and before the slides were completely dry, the filter sections were carefully peeled off. The cells were counterstained and mounted in a DAPI-mix, preparation see chapter preparations before lab work.

10.1.3. Microscopy and Evaluation

The filter sections were examined under a Zeiss Axiovision microscope equipped with a 100W Hg Lamp and appropriate filter set for DAPI, Alexa 488 and transmission light. Pictures were taken with the camera mounted on the Zeiss Axiovision microscope, analyzed with the Automatic Software and the counts for each picture manually controlled. Per station, depth and probe at least 400 DAPI-stained cells were counted and a minimum of 10 regions of interest (ROI) were analyzed. For each ROI, up to four different categories were enumerated: (1) total DAPI-stained cells, (2) DAPI-cells additionally stained with the specific probe and if applicable, cells surrounded by a silver grain halo (3) DAPI-cells and DAPI-probe-cells with silver grain halo around the cell

and (4) the area of the silver grain halo. The counting was performed and the percentages of the probe counts were calculated for each target and depth. The counting error, expressed as the percentage of standard error between replicates, was 25% for DAPI counts per mL and 7% for FISH counts. Negative control counts (hybridization with nonbacterial probe Non338) were always below 1% for FISH counts.

The statistical analysis was performed with SPSS 16.00. The data followed normal distribution and a one-way ANOVA was performed.

10.1.4. Chemicals and preparations before Lab work

PBS [10%]

For the phosphate buffered saline system (PBS) with the concentration of 10%, 2.76g sodium phosphate monobasic dihydrate [$\text{NaH}_2\text{PO}_4 \cdot 2\text{H}_2\text{O}$] (molecular weight (MW) $156.01 \text{ g mol}^{-1}$, Sigma-Aldrich), 14.24g sodium phosphate dibasic [Na_2HPO_4] (MW $141.96 \text{ g mol}^{-1}$, Sigma-Aldrich) and 75.97g sodium chloride [NaCl] (MW 58.44 g mol^{-1} , Carl Roth GmbH&Co.KG) were transferred into a 1L Schott flask, put on a magnet stirrer and the chemicals dissolved in 0.5 L fresh Milli-Q water. After the chemicals were dissolved, the pH was adjusted to 7.7, then the solution was filled up to 1L with fresh Milli-Q water, mixed and autoclaved. The PBS [10%] was kept as stock and the PBS [1%] was prepared fresh monthly with an adjusted pH ranging between 7.4 to 7.6.

EDTA [0.5M]

Ethylendiamintetraacetat (EDTA) was diluted to a 0.5M concentration. Therefore, 186.12g of EDTA (MW $372.24 \text{ g mol}^{-1}$, Sigma-Aldrich) were transferred into a 1L Schott flask, 0.5L fresh Milli-Q water was added and the flask was placed on a magnet stirrer. To enable the dissolution of the EDTA, the pH was adjusted to 8 by adding sodium hydroxide [NaOH] (MW 40 g mol^{-1} , Sigma-Aldrich) pastilles. When the chemicals were dissolved, the solution was made up to 1L, the pH of 8 controlled and the solution was autoclaved.

SDS [10%]

Sodium dodecyl sulphate (SDS) [$\text{CH}_3(\text{CH}_2)_{11}\text{OSO}_3\text{Na}$] (MW 288.38 g mol⁻¹, Sigma-Aldrich) was diluted in fresh Milli-Q water to a 10% concentration. Therefore, 50g of SDS were transferred into a 0.5L Schott flask and 0.4L fresh Milli-Q water was added. The flask was placed into a warm water bath (40°C) until the SDS was completely dissolved. Note that SDS must not be autoclaved, otherwise the organic compound SDS will degrade.

Tris-HCl [5M]

For the Tris-HCl [5M], 157.6 g tris(hydroxymethyl)aminomethane [$(\text{HOCH}_2)_3\text{CNH}_2$] (MW: 121.14 g mol⁻¹, Sigma-Aldrich) was transferred to a 1L Schott flask and 0.5L fresh Milli-Q water added. The pH was adjusted to 8 with hydrochloric acid [6M] [HCl] (MW: 36.46 g mol⁻¹, Carl Roth GmbH&Co.KG). When the chemical was dissolved, the solution was filled up to 1L and autoclaved.

NaCl [5M]

146.1 g sodium chloride [NaCl] (MW 58.44 g mol⁻¹, Carl Roth GmbH&Co.KG) were dissolved in 0.4L fresh Milli-Q water in a Schott flask. When the chemical was completely dissolved, the content was filled up to 0.5L and autoclaved.

HCl [5M], [0.1M]

To obtain the appropriate hydrochloric acid [HCl] (MW: 36.46 g mol⁻¹, Carl Roth GmbH&Co.KG) concentration, the amount of HCl was added into a certain amount of fresh Milli-Q water following the noted equation.

$$\text{HCl}_{\text{concentration given}} [\text{mol L}^{-1}] \times \text{HCl}_{\text{volume added}} [\text{L}] = \text{Volume}_{\text{wanted}} [\text{L}] \times \text{HCl}_{\text{Concentration wanted}} [\text{mol L}^{-1}]$$

Blocking reagent [10%]

Before the blocking reagent was mixed, the maleic acid buffer (MAB) was prepared. Therefore, 11.608 g maleic acid [$\text{HO}_2\text{CCHCHCO}_2\text{H}$] (MW: 116.08 g mol⁻¹, Sigma-Aldrich) were transferred into a 250 mL Erlenmeyer flask containing 80 mL fresh Milli-Q water, to obtain a concentration of 100mM and 8.766 g sodium chloride [NaCl] (MW 58.44 g mol⁻¹, Carl Roth GmbH&Co.KG) were added (150 mM final conc.). After the chemicals were dissolved, the pH was adjusted to 7.5 with

sodium hydroxide [NaOH] (MW 40 g mol⁻¹, Sigma-Aldrich) pastilles and afterwards the solution was filled up to 100 mL.

For the 10% blocking reagent, 10g blocking reagent (Boehring-Mannheim) were put into a 500mL Erlenmeyer flask and 80 mL of the previously prepared MAB added. The flask was put on a magnet-stirrer device heated up to 60°C, the flask lid was covered with aluminum foil and the blocking reagent slowly diluted under constant stirring for about 4h. Note that the blocking reagent must not be boiling during this procedure. When the blocking reagent was completely dissolved forming a thick and milky-white liquid, the solution was filled up to 100mL with MAB, properly mixed and autoclaved. Finally, the blocking reagent [10%] was aliquoted in 8 mL portions in 25 mL Greiner tubes, the rest was distributed in 1.5 mL Microfuge tubes. The tubes were stored frozen at -20°C and the microfuge tube in use was stored at 4°C. According to the specification of the manufacturer, the solution is good for a few days at 4°C and for many months stored frozen at -20°C.

Hybridization Buffer

For the hybridization, different hybridization buffers for the probes targeting the Bacteria and the bacterial clade SAR324, the bacterial cluster SAR11, SAR406, SAR202, NonEUB and for the probes targeting the archaeal divisions Crenarchaeota and Euryarchaeota were prepared at the beginning of the laboratory work and stored at -20°C.

The hybridization buffer was prepared in a 10mL Greiner tube. For all probe-specific hybridization buffers the following steps were identical. Dextran sulphate (Sigma-Aldrich), NaCl [5M], Tris-HCl [1M] and Triton[™] X-100 [100%] (Sigma-Aldrich) were added to the tube, for detailed volume and concentrations see table and for details on the chemicals see the chemical list. To dissolve the added chemicals, the tubes were placed in a water bath at 50°C for 30 min and afterwards, cooled down on ice.

Hybridization buffer:

Stock reagent	Volume	Final concentration
Dextran Sulfate	1g	10%
NaCl [5M]	1800 µL	900mM
Tris-HCl [1M]	200 µL	20mM
Triton [™] X-100 [100%]	5 µL	0,05%

To the cooled solution, 1000µL of blocking reagent [10%] and a certain amount of formamide [HCONH₂] (MW 45.04 g mol⁻¹, Sigma-Aldrich) was added to form the specific hybridization buffer, details see table below. The different formamide concentrations were added to ensure optimal stringency conditions of each probe to the target region of the rRNA at the uniform hybridization temperature of 35°C.

Hybridization buffer formamide concentrations:

Probe class	Formamide (Volume)	Final concentration (Formamide)
EUB388 (I-III) SAR324 (-625, helper) NonEUB	5500 µL	55%
SAR11 (-152R, -441R, -542R, -732R)	4500 µL	45%
SAR406 (-97)	6500 µL	65%
SAR202 (-104R, -312R)	4000 µL	40%
CREN (537, 554) EURY (806)	2000 µL	20%

The tubes were filled with sterile water up to 10mL and stirred with a sterile stick and vortexer until a homogenous solution was present. Afterwards the tubes were stored at -40°C.

Amplification buffer

The amplification buffer was prepared in a 10mL Greiner tube and consisted of dextran sulphate, NaCl [5M], blocking reagent [10%] and PBS [1x], detailed volumes and concentrations are given in the table below.

Amplifications buffer:

Stock reagent	Volume	Final concentration
Dextran sulphate	0.5 g	10%
NaCl [5M]	200 µL	2 M
Blocking reagent [10%]	50 µL	0,1%
PBS [1x]	fill up to 5 mL	

The reagents were stirred with a sterile stick and vortexed until a homogenous solution was obtained. Then, the solution was filtered through a 0.2 µm Acrodisc attached to a syringe into a

fresh 25mL Greiner tube. The amplification buffer was freshly prepared every week and kept at 4°C.

DAPI-MQ-mix

For the DAPI-MQ-mix, 1 μL of 4',6-diamidino-2-phenylindole (DAPI) [50 mg mL^{-1}] (Sigma-Aldrich Chemie BV) and 999 μL of fresh Milli-Q water were mixed in a light-tight 1.5 mL microfuge tube and kept at 4°C.

Vectashield-Citifluor-mix:

For the Vectashield-Citifluor-mix, Citifluor (Citifluor Ltd.), Vectashield (Vector Laboratories Inc.) and PBS [1x] were mixed in a cryovial, for detailed volumes and concentrations see table below. The tubes were wrapped in aluminum foil and stored at 4°C.

Stock reagent	Volume	Final concentration
Citifluor	1570 μL	55%
Vectrashield	285 μL	1%
PBS [1x]	145 μL	0.5%

DAPI-mix

The DAPI mix consisted of the same chemicals as used for the Vectashield-Citifluor-mix with addition of 4',6-diamidino-2-phenylindole (DAPI) [50 mg mL^{-1}] (Sigma-Aldrich Chemie BV), for detailed volumes and concentrations see table below. The mix was prepared in a cryovial, vortexed, the tube was wrapped in aluminum foil and stored at 4°C.

Stock reagent	Volume	Final concentration
Citifluor	1530 μL	55%
Vectrashield	280 μL	1%
PBS (1x)	140 μL	0.5%
DAPI [50 mg mL⁻¹]	40 μL	0,1 $\mu\text{g mL}^{-1}$

Photographic emulsion, developer and fixer

The photographic emulsion (autoradiography Emulsion Type NTB-2, Kodak) was melted in the dark in a water bath at 45°C for 1 h. Afterwards, the emulsion was mixed with ultrapure water (Sigma) in a 2:1 volume ratio, equal to the volume ratio of 7mL Sigma water to 3.5mL photographic emulsion. The emulsion was divided into small aliquots of 10.5 mL each, put in light-

tight vials and stored at 4°C. Each aliquot was melted only up to three times to avoid high background levels of silver grains.

The developer (Dektol developer, KODAK) and the fixer (fixer for filmes, plates and papers, KODAK) were prepared according to the specification of the manufacturer. The developer was dissolved overnight in 3L fresh Milli-Q water at room temperature in a 5L light-reduced Schott flask, while slowly stirring on a magnet stirrer. After the precipitate had dissolved, 0.8L fresh Milli-Q water was added and the stored in the dark.

The fixer was dissolved in 3L fresh Milli-Q water in a 5L light-reduced Schott flask at 37°C while slowly stirring on a magnet-stirrer set at 37°C. After the precipitate had dissolved, 0.8L fresh Milli-Q water was added and the solution stored in the dark.

Horseradish peroxidase probes (HRP Probes)

All the probes used for CARD-FISH and Micro-CARD-FISH were horseradish peroxidase probes (HRP probes) and were labelled with a horseradish peroxidase at the 5' termination of the oligonucleotide sequence of the probe. The HRP probes had a size range between 15-23 base pairs, (see table below) bound to an easily accessible complementary region on the rRNA of the target. The sequences of the different HRP probes had been reported previously, see table below, and were synthesized at Thermo Fisher Scientific.

The HRP probes were shipped in a dried state. Thus, the probes were more stable and could be stored below 4°C for up to one year. Before opening, the tubes were spun down as part of the content may have gotten stuck to the lid. To dissolve the dried probes, sterile water was added to obtain a 100-fold concentration, following the information specified by the manufacturer for each oligonucleotide probe shipped. The 100-fold concentrations were diluted to 10-fold concentrations, aliquoted in microfuge tubes holding 60µL and stored at -20°C. Before the addition of the sterile water and the aliquot, the sterile water and the Microfuge tubes were sterilized by UV- radiation for 0.5 h. The microfuge tubes holding the 1-fold concentration of the probe were only thawed once and kept in at 4°C in the dark for up to one week.

target	name of probe	sequence	published by
Bacteria	EUB338 I	GCTGCCTCCCGTAGGAGT	Amann et al. (1990)
	EUB338 II	GCAGCCACCCGTAGGTGT	Daims et al. (1999)
	EUB338 III	GCTGCCACCCGTAGGTGT	Daims et al. (1999)
SAR11	SAR11-152R	ATTAGCACAAAGTTTCCYCGTGT	Morris et al. (2002)
	SAR11-441R	TACAGTCATTTTCTTCCCGAC	Morris et al. (2002)
	SAR11-542R	TCCGAACTACGCTAGGTC	Morris et al. (2002)
	SAR11-732R	GTCAGTAATGATCCAGAAAGYTG	Morris et al. (2002)
SAR406	SAR406-97	CACCCGTTCCGCCAGTTTA	Fuchs et al. (2005)
SAR324	SAR324-625	CGAAAGACCCTCCGG	Wright et al. (1997)
	helper	GGTTGAGCCCCGGGCTTTCACC	Fuchs (2012, E-mail)
SAR202	SAR202-104R	GTTACTCAGCCGTCTGCC	Morris et al. (2004)
	SAR202-312R	TGTCTCAGTCCCCCTCTG	Morris et al. (2004)
Crenarchaea	CREN537	TGACCACTTGAGGTGCTG	Teira et al. (2004)
	CREN554	TTAGGCCCAATAATCMTCT	Woebken 2007 AEM
Euryarcheota	EURY806	CACAGCGTTTACACCTAG	Teira et al. (2004)
NonEUB	EUB338	ACTCCTACGGGAGGCAGC	Manz et al. (1992)

List chemicals

Product	Description	Company	Art.Nr.:	Size
Agarose	low melting-point sea plaque GTGagarose	FMC bioProducts	56111	
Aspartic acid	D-[2,33-H]	Amersham Bioscience	Nr.: TRK606	250µCi
Aspartic acid	L-[2,33-H]	Amersham Bioscience	Nr.: TRK574	1mCi
Blocking Reagent	Boehringer Mannheim Blocking reagent	Roche Diagnostics GmbH (NL)	1-096-176	50g
Buechner funnel	(diam.59mm)	VWR International	HALD127C/1	
Citifluor	Glycerol- PBS solution	Citifluor Ltd.	AF1	25ml
DAPI	DAPI stain	Sigma-Aldrich Chemie BV	D9564	1x10mg
Dextran Sulfate		Sigma-Aldrich Chemie BV	D8906	100g
Dispensette	0.5-5ml	Sigma-Aldrich Chemie BV (NIOZ:Brand)	Z33,194-5 (07 X5250?)	
DMF	NN-Dimethyl formamide	Sigma-Aldrich Chemie BV	D4551	250ml
EDTA		Plusone	17-1324-01	
FISHprobes		Thermo Electron Corporation Biopolymers		
Formamide	(Fluka)	Sigma-Aldrich Chemie BV	47671	1l 250ml
Glascribe		Bel-Art Products, Inc. Scienceware	H441500000	
H2O2	30% (w/w)	Sigma-Aldrich Chemie BV	H1009	5ml
Kodak Dektol Developer		Sigma-Aldrich Chemie BV	P6917	1GA
Kodak Fixer		Sigma-Aldrich Chemie BV	P6557	1GA
Kodak NBT-2		Integra Biosciences GmbH	IB-01433	1x
Lysozyme	from chicken egg,white	Sigma-Aldrich Chemie BV	Nr.: L7651	50000 units/mg 25g
maleic acid		Sigma-Aldrich Chemie BV	M-0375	500g

multiwell plates	12-well (TC treated with lid)	Sigma-Aldrich Chemie BV	M 8687	1St.
Nitrocellulosefilter	0.45µm 25mm(diam.)	Sigma- AldrichChemie BV	N9020	100EA
Paraformaldehyde		Sigma-Aldrich Chemie BV	Nr.: P6148	1x500g
Polycarbonate filter	0.2µm 25mm(diam.)	Millipore	GTTP	100
Proteinase K	(Fluka) from triturachium album	Sigma-Aldrich Chemie BV	P4850	1x1ml
Safetylight	Dunkel kammer leuchte 230V,50Hz	Kaiser Fototechnik	Nr.: 4018	
Safetylight	lamp model B	Eastman Kodak Company	141-2212	
Safetylight filter	Dunkel kammer filter (rot) 9x12cm	Hama	Nr.:8194	
Safetylight filter	Kodak 2 darkred	Eastman Kodak Company	152-1525	
SDS	Lauryl Sulfate	Sigma-Aldrich Chemie BV	L-4509	100g
2 slide mailer	tubes for emulsion	Raymond A Lamb Limited	Nr.:E6.2	125x
staining dishes		Sigma-Aldrich Chemie BV	S4642	2x3
staining dishes	slide rack	Sigma-Aldrich Chemie BV	S5017	1.1.1.1.1 1x3
staining dishes	rack handle	Sigma-Aldrich Chemie BV	S5142	1x3
TEA	Triethyl amine	Sigma-Aldrich Chemie BV	17924	
TRIS		Plusone	17-1321-01	
Triton X100	X-100	Sigma-Aldrich Chemie BV		500ml
Tyramide dye	Alexa Fluor 488 succinimidyl ester	Molecular Probes Europe BV	Nr.: A-20000	1x1mg
Tyramide dye	Alexa Fluor 555 succinimidyl ester	Molecular Probes Europe BV	Nr.: A-20009	1x1mg

TYR-HCl	Tyramine-HCl	Sigma-Aldrich Chemie BV	T2879	5g
Vectashield		Vector Laboratories, Inc.	H-1000	10ml
Water	Sigma Water	Sigma-Aldrich Chemie BV	W4502	1L

10.2. Curriculum Vitae

Lebenslauf

Franziska Maria Eibenberger

Ausbildung

1992/93	Vorschule Maurer-Lange-Gasse
1993/94 - 1996/97	Volksschule Maurer-Lange-Gasse
1997/98 - 2000/01	Unterstufe Gymnasium St. Ursula
2001/02 - 2004/05	Oberstufenrealgymnasium St. Ursula
Mai 2006	Matura
Sept. 2005	Studium Biologie-Ökologie
Feb. 2010	Bachelor of Science
März 2010	Masterstudium Ökologie-Meeresbiologie
Jan.-Sept 2011	Erasmussemester Lissabon, Portugal
Mai 2013	Master of Science

Praktika

Sommer 2008	Volontariat Nationalpark Hohe Tauern
2008-2001	Mitarbeiterin Tiergarten Schönbrunn
2009	Mitarbeiterin Haus des Meers Wien
Mai 2010	Übungen rezente und fossile Korallenriffe, Ägypten
Juli 2010	Schildkrötenpraktikum, Türkei
Sept. 2010	Meeresbiologisches Spezialpraktikum, Corsica
2011	Universitätsprojekt, Portugal
2011	Forschungsreise Atlantik